Exploiting Radio Irregularity in Wireless Networks for Automated People Counting

by

Wei-Chuan Lin

A thesis
submitted to the Victoria University of Wellington
in fulfilment of the
requirements for the degree of
Master of Engineering
in Network Engineering.

Victoria University of Wellington
2013

Abstract

Wireless devices exist almost everywhere in our daily life. Wireless communications, which is an integral part of wireless devices, suffers from *radio irregularity* – a phenomenon referring to radio waves being selectively absorbed, reflected or scattered by objects in their paths, e.g., human bodies that comprises liquid, bone and flesh. *Radio irregularity* is often treated as a major challenge for wireless communication. However, we aim to take advantage of the phenomenon of *radio irregularity* to provide a cost-effective approach for automated people counting. People counting is extensively used for intelligence-gathering to be used in forecasting, resource allocation and safety-related applications 2like crowd control. Existing people counting techniques use light, infrared, or thermal energy for human movement detection. However there have major limitations, for example the visible light camera and infrared sensors do not penetrate smoke or obstacles such as wall and furniture. Also, a large deployment of these devices is costly owing to the use of specialized sensors.

We propose an automated people counting system using the radio irregularity phenomenon of existing wireless infrastructure with minimal additional hardware and installation costs. This thesis presents an experimental study to demonstrate how radio signal fluctuations arising from radio irregularity can be used to provide a simple low-cost alternative to dedicated sensing systems for indoor automated people counting. Firstly, we study the effect on received signal strength with human motion interference on radio signals. Then we propose and evaluate the performance of three approaches, namely, overcomplete dictionary based pattern recognition (OCPR) approach, probability density approach and standard deviation approach. With high accuracy of motion detection, we then focus

on the design of automated people counting system using the proposed detection approach. To differentiate the number of people, we apply discriminant analysis which is a statistical method to perform classification based on independent variables. We validated the proposed people counting system by conducting experiments under both controlled and uncontrolled environments and show that we are able to achieve high accuracy in counting up to five people in groups with no specific formation.

Acknowledgments

First of all, I heartily appreciate the help from my supervisors, Prof. Winston Seah and Dr. Wei Li, for their encouragement, guidance and support from the beginning to the very end. Winston and Wei have been extremely helpful supervisors both technically and psychologically. This work would not have been possible without them. I consider myself extremely lucky and blessed to have the chance to work with such helpful supervisors.

Wireless Network Lab has been an absolutely brilliant environment to perform research as well as working with team members. I appreciate the friendship and support from other graduate students in Wireless Network Lab at the Victoria University of Wellington: Nan Liu, Xia Dong, Casimirraj Subramanian, Noorfarha Ngabas and Muhammad Mahmood. With their unique skills and personalities, it is a pleasure to work with them. I would like to express my special appreciation to Min Sun, ShaoAn Yen, Casimirraj Subramanian, OnKit Chan and CheukHim Lee. They selflessly agreed to be the target objects to conduct detection experiments under a controlled environment.

Lastly, and most importantly, I would like to express my appreciation to my family and friends. My parents, ChengFu Lin and ChenHui Hsu, have given me opportunities to study aboard and accomplish this educational goal. WeiChen, my brother has always been the key supporter during my studies. WenShan Lee has been particularly supportive and encouraging. I cannot thank you enough for your support and love dur-

ing my studies.

Contents

List of Figures

List of Tables

Chapter 1

Introduction

Wireless communication and devices have grown to become an integral part of our daily life, like the Internet, which has grown into a large cyber-physical system that connects not just computer systems but a plethora of systems, devices, sensors and objects. The technologies extend beyond computation and communication, to identification and tracking, sensing and actuation, and even intelligence and cognition. Ensuring connectivity is increasingly reliant on wireless communications as connected devices become more ubiquitous and embedded into our daily living space. Unfortunately, wireless communication suffers from *radio irregularity* – a phenomenon referring to radio waves being selectively absorbed, reflected or scattered by objects in their paths, e.g., human body that comprises liquid, bone and flesh. *Radio irregularity* is often treated as a major challenge for wireless communication. However, we aim to take advantage of *radio irregularity*, and by exploiting the existing wireless communication infrastructure, provide a cost-effective approach for automated people counting.

People counting is extensively used in different industries, including retail (stores, malls and shopping centres), colleges and universities, government facilities, government non-profit organizations, visitor centres, libraries, museums and art galleries. In the retail industry, it is a form of intelligence-gathering that helps a retailer determine the percentage of visitors who actually make purchases. This is a key performance indicator of a store's performance as compared to just looking at the sales data. It also helps the management to optimize the usage of staff resources, e.g. deploy more staff during peak periods and cutting down during lull periods in order to save wages. Pedestrian traffic data can also help to evaluate advertising and promotional campaigns. Retail management can assess the effectiveness of advertising campaigns by examining how the traffic has responded to it. Queue management can also be optimized by utilizing the pedestrian traffic data. Operational efficiency and profitability can be enhanced by people counting systems. For building automation and management purposes, people counting is used to optimize the use of resources as well as ensure that a safe level of occupancy is maintained. Automated people counting cannot tolerate false positives that result in overcounting, giving inaccurate data that are used for forecasting and resource allocation.

1.1 Problems in Tracking and Automated People Counting

Currently, most of the applications for inferring human movement are achieved by using light, infrared, or thermal energy. However, these inferring technologies have some major limitations. Visible light cameras largely depend on the intensity of light and the colour of the background in order to differentiate human from the video. In addition, light and infrard do not penetrate smoke and obstacles such as wall or furniture. These drawbacks limit the usability and suitability of light and infrard in emergency environment such as a smoke-filled building. Thermal imaging based detection requires specialized sensors which are expensive. The accuracy of detection can be degraded by the lack of colour and texture information from thermal image. Large deployment of these devices is impractical due to their high cost and obtrusive characteristics.

Unlike the detection technologies discussed above, radio-frequency (RF) electromagnetic waves can penetrate wall and smoke. Radio signals, however, may be reflected, diffracted and/or scattered in the channel [2]. Two components of signal propagation considered to be key causes of radio irregularity are path loss and transmission power [3]. The impact of radio irregularity depends on the obstacles and the wireless signals transmitted. The human body selectively reflects, diffracts, and scatters radio signals such that the radio irregularity varies over time. Consequently, the received signal strength at the receiver fluctuates. Radio irregularity which has often been viewed as a problem can instead be exploited for automated people counting with minimal additional hardware and installation costs. However, the degree of radio irregularity is largely dependent on the environment.

1.2 Objectives

In this thesis, we focus on automated people counting design through studying the characteristic of RF signals. The ultimate objective of this thesis is to realize an automated people counting system which uses RF signals as an indicator. There are three goals in this thesis:

1. Study and analyse the characteristics of RF signal fluctuations due to the occurrence of human movement in the wireless environment.

2. Design movement inferring algorithms based on the signal fluctuation cause by human movement.

3. Realize the automated people counting system by extending the movement detection algorithm and applying discriminant analysis to differentiate the signal fluctuation patterns caused by different numbers of people.

1.3 Contributions

The overall contribution of this thesis is realizing the automated people counting system using the fluctuation of RF signals causing by human movement. The following lists the major contributions of this work:

- Experimental analysis of the characteristics of RF signal fluctuations caused by human interference.

- Three movement detection algorithms have been proposed and implemented, namely, overcomplete dictionary based pattern recognition technique [4], probability density approach [5] and standard deviation approach [6]. The proposed detection algorithms have been validated and evaluated through experimental studies under a controlled environment.

- An automated people counting system has been realized by applying a statistical classification method, namely, *discriminant analysis*. A series of experiments, under controlled and uncontrolled environments, have been conducted and the scheme has been shown to achieve high accuracy in counting up to five people in groups with no specific formation [6].

1.4 Thesis Structure

The structure of the thesis is as follows:

- Chapter 2 provides background and related works on detection approaches and people counting methods.

- Chapter 3 Discusses and explains the design of the proposed detection algorithms, starting with explaining the use of RSSI fluctuations.

- Chapter 4 presents detection results based on single-transmitter and single-receiver configuration and discusses the performance of each detection approach in terms of detection accuracy, latency of detection, and the occurrence of false-positives.

- Chapter 5 discusses the hardware specification of wireless sensor nodes used in the experiment and the effect on detection accuracy of various factors.

- Chapter 6 introduces our conceptual model of sensor placement followed by the single-transmitter multiple-receivers configuration and the *discriminant analysis* technique to differentiate the number of people under controlled and uncontrolled environments.

- Chapter 7 contains conclusion and sugguestion for future work.

- Appendix A describes and discusses the steps that are required to process the RSSI readings and apply discriminant analysis using the SPSS software [7].

Chapter 2

Related Work

The ability to locate people is extremely valuable. Widespread usage of people counting has fed the growth of commercially available automated people counting technology, among which infrared (IR) beam counters, thermal counters and video/CCTV cameras are most often used. In addition, Global Positioning System (GPS), real-time location systems (RTLS), radio frequency identification (RFID) are also widely used for locating target objects. These target objects will need to attach or carry a device to be locatable. In contrast, device-free localization (DFL) is the practice of locating object without using tag or device on the target objects. In this chapter, we provide an overview of the human detection and people counting techniques, that have been developed, published and/or commercially available.

2.1 Reason for Use

The knowledge of location of target objects can be used by many applications such as automated people counting system. There are various reasons to implement people counting systems and several ways to utilize the information.

Retail

The automated people counting system is a key for retail analytics. It is crucial information for the management of retail stores to utilize during business decision making. *Conversion Ratio* is the key metric that can be derived using the automated people counting system. Conversion ratio is calculated as the ratio of number of purchasers to the total number of people entering the shop. This indicator helps the management in the decision making and strategy planning process. Store managements rely on the visitor statistics to measure the effectiveness of their marketing.

Occupancy

For building safety, public locations are often designed to hold a specific number of people. An accurate people counting system is essential to track the number of people within an area and provide precise measures to ensure the safety of the building.

2.2 Sensor Technologies

The usage of different types of sensor technology is dependent on the needs of applications. We discuss the common usages in DFL system and their advantages and disadvantages in the following subsections.

Infrared

The simplest and possibly cheapest approach is a single-beam IR counter placed across an entrance. However, such a counter suffers from numerous drawbacks and is only suitable detecting someone passing, e.g. entering/leaving a shop. These commonly used counters have very high percentage of errors when multiple persons cross their monitoring area at a time. When multiple (IR) beams or other forms of boundary sensors are deployed with careful placements strategies and coupled with artificial intelligence and/or analytical techniques for processing, a more accurate and versatile people counting system can be realized [8, 9].

Thermal Imaging

People counters that use thermal imaging are typically mounted overhead and have the ability to simultaneously maintain separate counts for multiple people moving in two directions (in and/or out). Thermal imaging is a widely used technology for many applications, especially by law enforcement agencies and the military. The IR images captured by the heat detectors are then processed to determine the number of people [10]. A major advantage of the thermal imaging detection and people counting system is that the heat detector does not require visible light to achieve visibility on targeted objects. In addition, there is no privacy concern since individuals are not identifiable. However, there are also disadvantages such as limited view angles and high financial costs. There are a few commercial products using infrared thermal imaging technology, e.g., Traf-Sys thermal sensor [11] and IRISYS [12].

Optical Cameras

Video-based people counters work on video streams obtained through video/CCTV cameras which are then run through intelligent video processing techniques to identify and count the people in the video. The key limitation of optical cameras is that they cannot penetrate obstructions. The ability of detecting objects can be severely affected when obstructions block the line-of-sight (LOS) between the camera and the target object. The accuracy of such approaches can vary according to the level of ambient lighting and background colour contrasts [13]. Hybrid approaches combining IR and video cameras, together with neural networks, have been proposed to improve the accuracy of visual-based automated people counting [14]. Also, in comparison to thermal imaging technology, privacy is a major concern when using optical cameras as the identities of individuals are recorded by cameras. The CountWise people counting system [15] utilises this technology to achieve people counting.

2.3 Radio Frequency DFL Technologies

Radio frequency device-free localisation is achieved by measuring and monitoring properties of the radio channel between pairs of wireless sensor nodes. The changes of wireless properties provide indications and information about the position of objects in the wireless environments. In the rest of the section, we will discuss various radio channel measurements for DFL with their strength and weakness.

2.3.1 Ultra-Wide Band (UWB)

UWB receivers have the ability to measure the amplitudes, time delays and phases of the multipath signals in the radio channel. The ability to measure the time delay of multipath signals gives UWB receivers crucial information about the positions of objects. The Channel impulse response(CIR) can be measured upon receiving a UWB pulse by a UWB transceiver. The CIR at time t can be represented as

$$h(t,\tau) = \sum_{i=1}^{N(t)} \alpha_i(t)\delta(\tau - \tau_i(t)) \tag{2.1}$$

$$N(t) = \text{Multipath components}$$
$$\alpha_i(t) = \text{Amplitude gain of } i\text{th component}$$
$$\tau_i(t) = \text{Time delay of } i\text{th component}$$

The spatial information of objects can be known by comparing the time delay $\tau_i(t)$ with LOS time delay. However, a calibration phase is needed for different environments to measure primary properties of existing RF channel such as LOS time delay. Furthermore, a limitation of using UWB transceivers is that they are certainly more expensive than narrowband transceivers.

2.3.2 Narrowband

Unlike UWB transceivers, narrowband transceivers cannot provide information regarding signal multipath components, but only have the ability to signal magnitude and phase at one frequency. The benefits of narrowband transceivers is that they are small in size and inexpensive. The benefits of low cost become a essential part for large deployment of RF sensor networks.

Received Signal Strength (RSS)

It was first reported in [16] that the shadowing effect caused by an object moving between two communicating wireless devices can be used for detection purposes. In particular, a human body comprises liquid, bone and flesh, that selectively absorb, reflect or scatter RF signals, leading to the phenomenon known as *radio irregularity*; radio irregularity leads to Received Signal Strength (RSS) fluctuation. Received Signal Strength Indication (RSSI) is a measurement received signal power in decibel terms. RSSI is calculated as follow:

$$R_{\text{dB}} = 20\,\log_{10}|\tilde{V}| = P_{\text{T}} + 20\,\log_{10}\left|\sum_{i=1}^{N}\alpha_i(t)\right| \tag{2.2}$$

where P_{T} is the transmitted power in dB

This phenomenon has been extensively used for device-free localization in wireless networks [17]. Radio Tomographic Imaging [18] measures the attenuation of signals across wireless links between many pairs of nodes in a wireless network to create images of objects moving within the network area. The variance of the measured RSS on the links in a network has also been used to infer the locations of people or objects moving in the network deployment area [19]. This approach utilizes a statistical model for the RSS variance as a function of a person's position with respect to the transmitter and receiver locations. The approach adopted by [16] has also been extended in [20] for outdoor people counting by measuring the RSS level measured at the receiver. The reliance on (absolute) RSS values, however, has a drawback during deployment, which is the need to take into consideration the channel model and other related factors like the impact of path loss and fading. These approaches also require complex signal processing techniques and a calibration phase for each deployment environment, and this can significantly affect the ease of deployment.

It has been observed in [1] that human movement through the path of the radio signal causes the histogram of the absolute RSS values to become more spread; this is manifested quantitatively as higher standard deviation. However, the standard deviation varies significantly across environments, making it difficult to define a universal threshold to detect movement in terms of these first order statistics. While also exploiting the RSS spread caused by human movement, the approach adopted in [1] focused on the fluctuation in signal strength instead, in order to reduce the impact of channel models and other environmental factors. However, there are false positives reported in their results which are deemed to be acceptable in the intrusion detection application considered in that work.

2.4 Summary and justification

In this thesis, we propose a network-oriented approach that utilizes RSS information of received packets to detect and count people when they cross the signal transmission paths. This information can be easily obtained from device drivers of wireless network interfaces when the packets are received and the goal of our approach is to be able to easily utilize the existing wireless transmitters and receivers already deployed in the environment.

Table 2.1 below highlights the core advantages of our proposed system over other people counting systems. We aim to maximize the level of detection accuracy using the existing wireless infrastructure without additional hardware and costs. In the next chapter, we present our human motion detection scheme using different ways of interpreting the radio irregularity phenomenon.

Detection Approach	Privacy Concern	Environment Dependant	Multiple People Detection	Costs
Infrared	**No**	**Yes**	**No**	**Low**
Thermal Imaging	**No**	**No**	**Yes**	**High**
Optical Camera	**Yes**	**Yes**	**Yes**	**High**
RF-based	**No**	**Yes**, Absolute RSSI	**Yes**	**High**
Proposed	**No**	**No**, RSSI Fluctuation	**Yes**	**Low**

Table 2.1: Comparison between proposed system and others

Chapter 3

Motion Detection Algorithm

In this chapter, we discuss the design of motion detection approaches using different approaches of interpreting the RSS fluctuations arising from radio irregularity. The three approaches used are: overcomplete dictionary based pattern recognition (OCPR) approach [4], probability density approach [5] and standard deviation approach [6].

3.1 RSSI Fluctuations

Most, if not all of the approaches that rely on the changes in RSS levels caused by human motion across the signal transmission paths require complex signal processing techniques and a calibration phase for each deployment environment. This significantly affects the ease of deployment.

In our scheme, we adopt a network-oriented approach that relies on RSS information of received packets which can be easily obtained from device drivers of wireless network interfaces when the packets are received. A key goal of our approach is to be able to utilize the existing wireless transmitters and receivers deployed in the environment without the need for accurate channel models nor complex signal processing techniques. We extend the method of using Received Signal Strength Indicator (RSSI) fluctuations proposed in [1] which has shown that two consistent patterns of RSSI fluctuations can be observed for two key scenarios of interest to us, namely, without human movement and with human movement across the signal transmission path, as shown in Fig. 3.1. For a given packet p_i, the RSSI fluctuation were calculated as $F(p_i) = S(p_i) - S(p_{i-1})$. For example, the sequence of RSSI values 1, 2, 4, 5, 8, 7, 6 produces the RSSI fluctuation values 0, +1, +2, +1, +3, -1, -1.

The histogram of RSSI fluctuations derived from the readings shows narrower distribution when there is no human movement across the signal path, i.e., less fluctuation across RSSI readings (Fig. 3.1a) and, conversely, signals fluctuate more in the presence of human movement resulting in the spread out distribution shown in Fig. 3.1b. In a setup inside a 8m$\times$6m room, with transmitter-receiver separation of 3 metres at a height of 1.2 metres, the absolute RSSI readings for packets recorded at the receiver over time is shown in Fig. 3.2. From the absolute RSSI readings, the fluctuation of RSSI readings is calculated, as shown in Fig. 3.3.

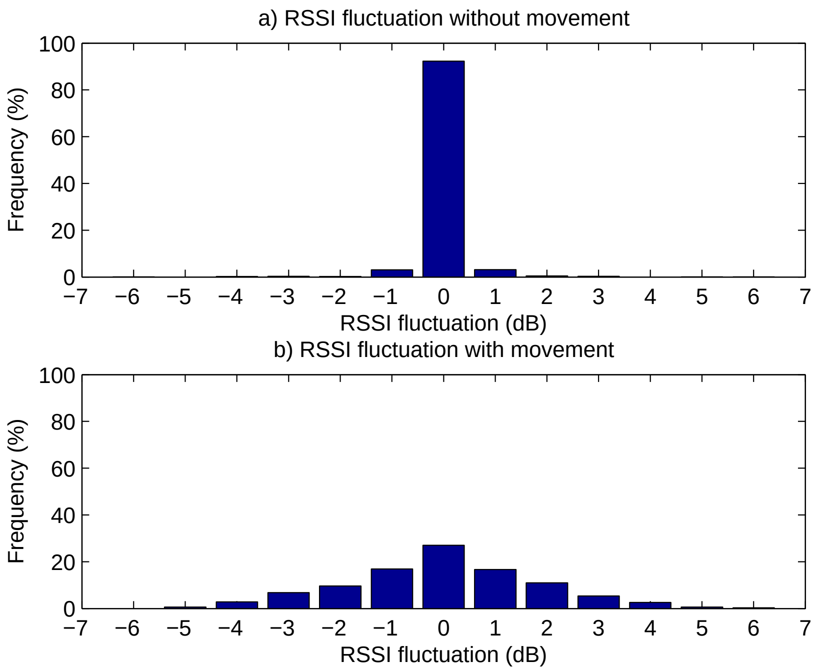

Figure 3.1: RSSI Fluctuation Patterns [1]

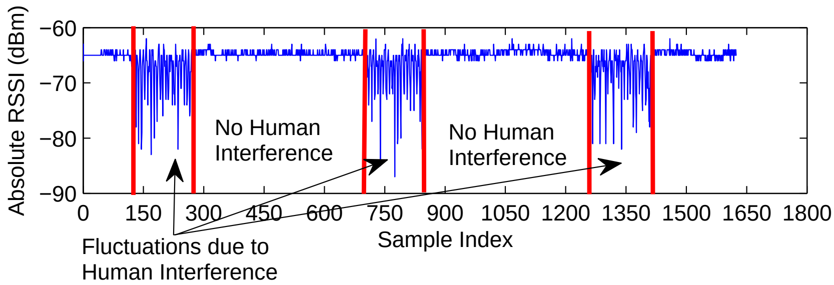

Figure 3.2: Absolute RSSI reading

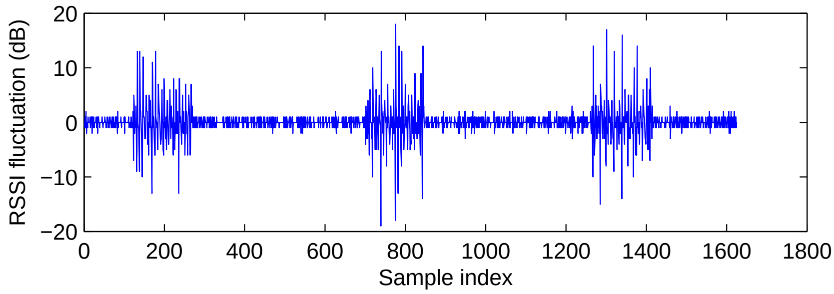

Figure 3.3: RSSI Fluctuation

3.2 Overcomplete Dictionary Based Approach

In this section, we present a movement detection system using an *overcomplete dictionary based pattern recognition* (OCPR) algorithm. This detection algorithm has been employed in ultra-wideband communications systems [21].

A flowchart of the proposed system is shown in Fig. 3.4a. It begins with the measured RSSI readings and calculates the frequency of RSSI fluctuations over a window of N packets. The overcomplete dictionary based pattern recognition algorithm takes this frequency data as input. The pattern recognition algorithm is shown in Fig. 3.4b.

The overcomplete dictionary $\mathbf{D}_N$ consists of two matrices

$$\mathbf{D}_N = [\mathbf{I} \;\; \mathbf{H}] \,, \tag{3.1}$$

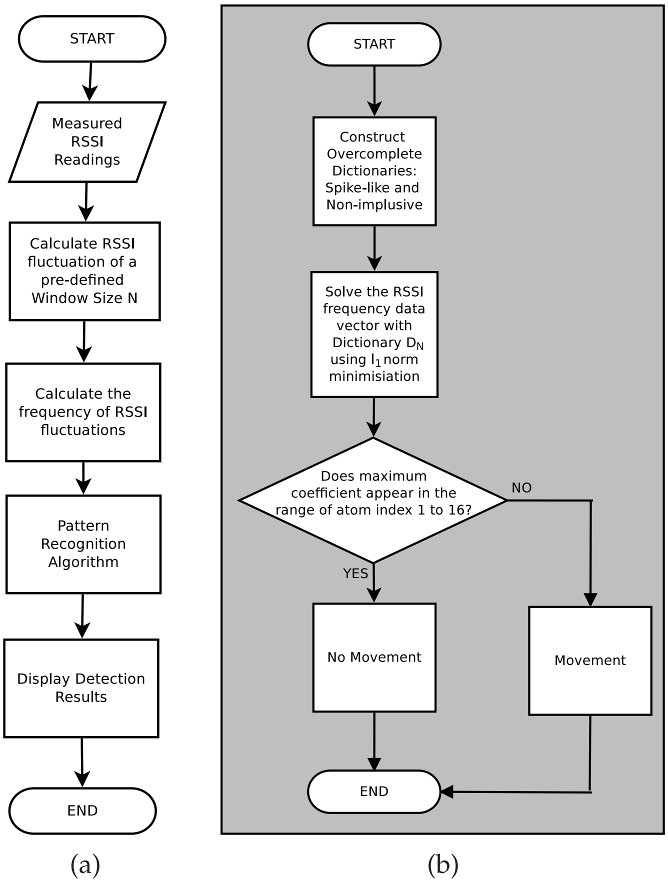

Figure 3.4: (a) Flowchart of the proposed movement detection system. (b) The overcomplete dictionary based pattern recognition

where

I is the spike-like dictionary with size of 16 x 16, and

H is the Walsh noise dictionary with size of 16 x 16.

The reason behind using Walsh noise dictionary is due to its non spike-like characteristic. The algorithm decomposes the RSSI frequency data vector y with dictionary $\mathbf{D}_N$ using l_1 norm minimisation [22][23] to obtain the solution

$$\mathbf{x} = \begin{bmatrix} \gamma_{\mathbf{I}} \\ \gamma_{\mathbf{H}} \end{bmatrix} \tag{3.2}$$

where

$$\mathbf{y} = \mathbf{D}_N\mathbf{x} = \mathbf{I}\gamma_{\mathbf{I}} + \mathbf{H}\gamma_{\mathbf{H}}, \tag{3.3}$$

The RSSI fluctuations patterns shown in Fig. 3.1 were decomposed with dictionary D_N using l_1 norm minimisation. The results with and without movement are shown in the Fig. 3.5. Atom indices 1 to 16 correspond to the spike-like dictionary and 17 to 32 to the Walsh dictionary. Fig. 3.5 clearly shows that the maximum coefficient lies between atom 1 to 16 when there is no movement, and between 17 to 32 when movement occurs. Thus the decision rule is that there is no movement when the largest peak is located between atoms 1 to 16, and movement otherwise.

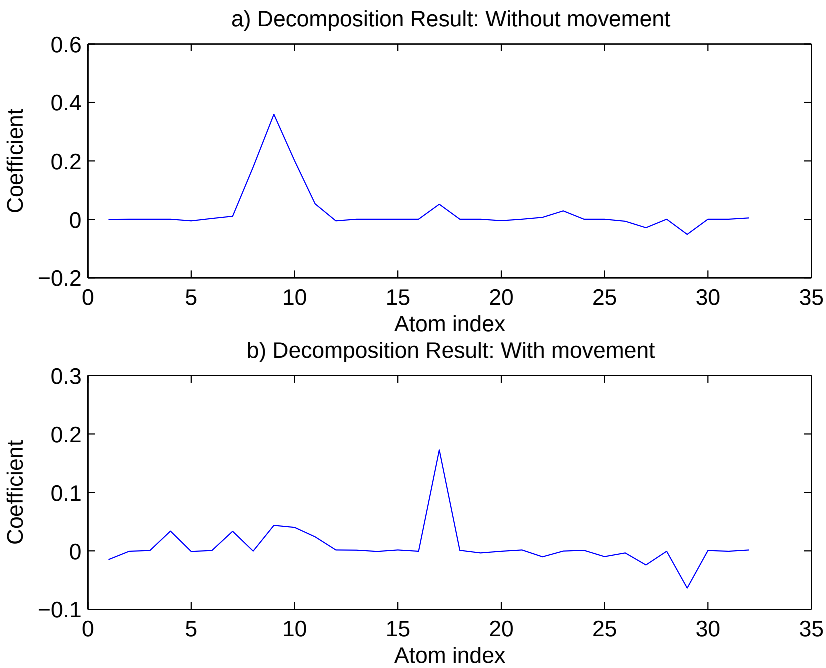

Figure 3.5: The dictionary based decomposition results.

We applied the overcomplete dictionary based approach to the dataset in Fig 3.2. The inferring results is shown in Fig. 3.6.

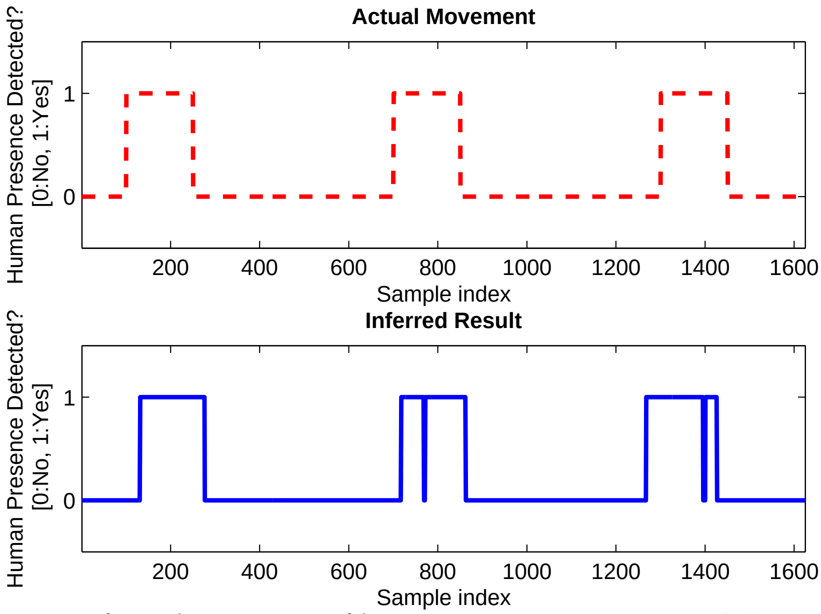

Figure 3.6: Inferred presence of human movement using OCPR approach

3.3 Probability Density Approach

Probability Density approach aims to utilize the probability of RSSI fluctuation within [-1, 1] as a movement indicator. According to the RSSI fluctuation patterns [1], the frequency of RSSI fluctuation between [-1, 1] is higher in the presence of movement. In other words, we can infer the presence of movement if the probability of RSSI fluctuation between [-1, 1] is high. We applied the probability density approach to the dataset 3.2. We then define a sliding window of N samples, where N is a parameter that can be tuned to achieve the desired accuracy for the target environment. In our example, a sliding window of size $N = 10$ is used to observe the behaviour of the RSSI fluctuation. Therefore, a window of RSSI fluctuations at sample 200 is shown in Fig. 3.7.

At sample 200, using the window of 10 previous readings, the mean and standard deviation are computed as 0.2727 and 4.6280 respectively. We then map the RSSI fluctuations into the normal distribution with the mean and standard deviation for that window, i.e. $\mu = 0.2727$ and $\sigma = 4.6280$, as shown in Fig. 3.8a representing the case where the signal has been subjected to interference by human movement across its path. Similarly, the normal distribution of RSSI fluctuation at sample 600, where there is no movement, is shown for comparison in Fig. 3.8b.

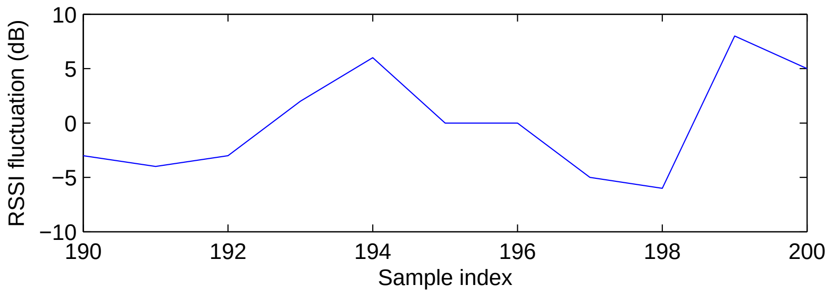

Figure 3.7: RSSI fluctuations over a window size of 10

From the graphs, we compute the probability of the RSSI fluctuation falling within the range [-1,1] (i.e. area under the curve from -1 to 1) to be 0.17078 for the case where there is movement across the signal path (i.e. sample 200) and 0.84303 for the case where there is no movement (sample 600). For the dataset shown in Fig. 3.2, we compute the probability of falling within the fluctuate range [-1,1] and plot the results as shown in Fig. 3.9. As shown, the probability of fluctuations falling in the range of [-1, 1] is below 0.3 in the presence of human movement. Hence, a probability value that is higher than 0.3 implies no human movement. Based on this threshold, we then infer from the results whether or not there has been human movement across the signal path, and the results are shown in Fig. 3.10.

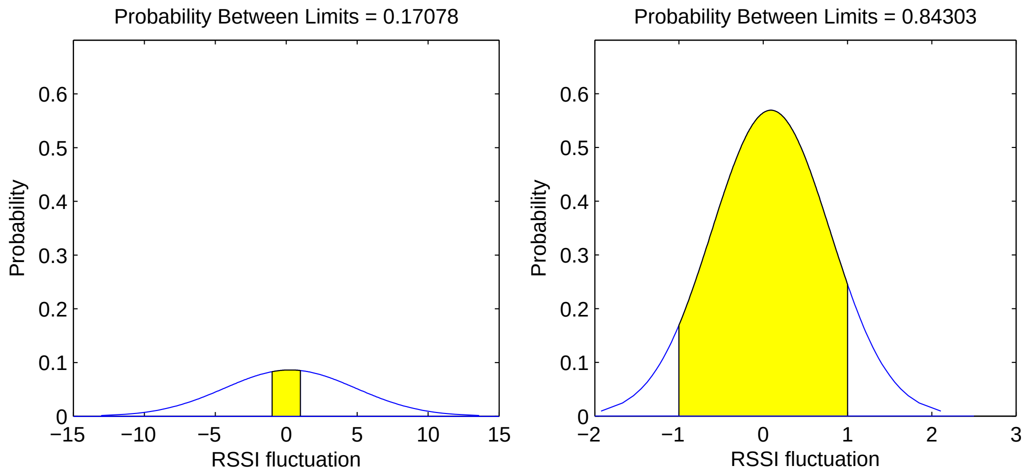

(a) Sample 200 (movement) (b) Sample 600 (no movement)

Figure 3.8: Normal distribution showing probability in fluctuation range [-1,1]

3.4 Standard Deviation of RSSI Fluctuation Approach

Using the probability density function of RSSI fluctuations falling within the range [-1,+1] as the threshold to signify no human movement has eliminated the occurrence of false positives [5], but it disregards information from the distribution of RSSI fluctuations that lie outside the region be-

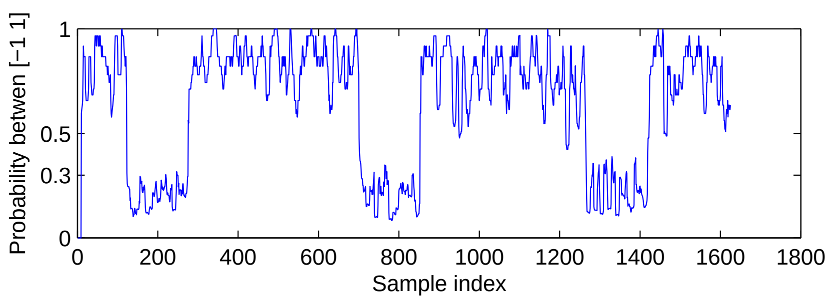

Figure 3.9: Probability of fluctuation within [-1,1] in Fig.3.2

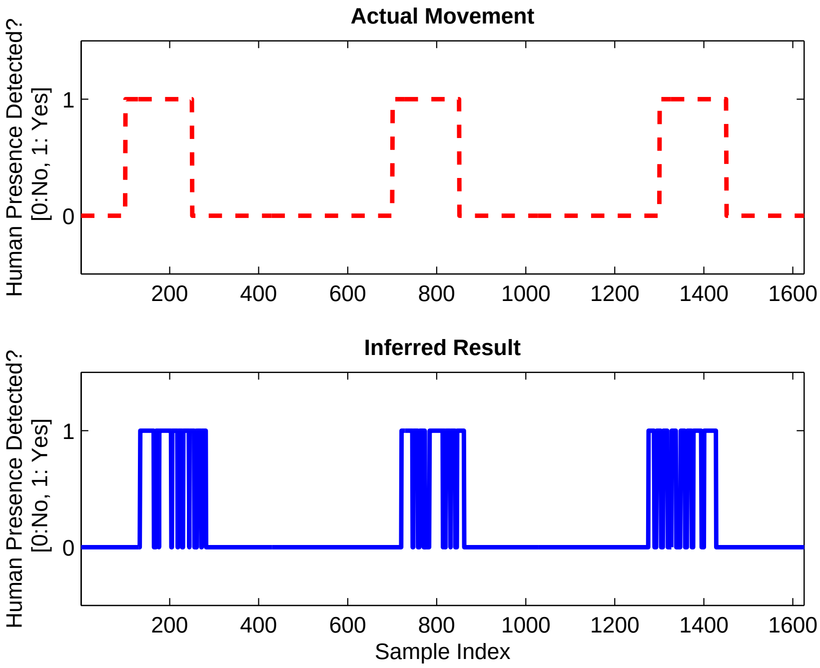

Figure 3.10: Inferred presence of human movement using PDF approach

tween -1 and +1. This is undesirable as the distribution of RSSI fluctuations has been shown to be a good indication of the size or crowd density of moving objects [24]. In order to enhance the ability of people counting using RSSI fluctuation, we observe the behaviour of the standard deviation of RSSI fluctuation. In the standard deviation detection approach, we compute the standard deviation of samples within a sliding window.

As shown in Fig. 3.13, we use a sliding window of size $N = 10$ to observe the behaviour of RSSI fluctuation. Signal interference due to human motion causes rapid RSSI fluctuations which results in an increased standard deviation. For the dataset shown in Fig. 3.2, we compute the standard deviation of the RSSI fluctuation and the computed results are shown in Fig. 3.11; at sample 200 (human presence), the standard deviation (of the most recent 10 RSSI fluctuation readings) is 4.6280 and at sample 600 (no human presence), the standard deviation is 0.6325. The standard deviation of RSSI fluctuations being higher than 2 implies the

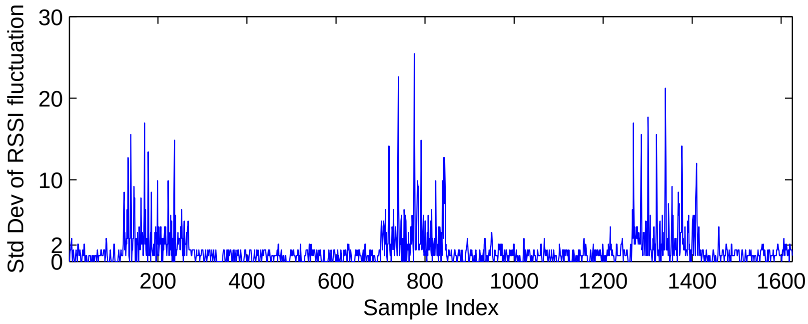

Figure 3.11: Standard Deviation of fluctuation for RSSI readings in Fig.3.2

presence of human movement, which provides a clearer threshold than the approach presented in [5]. We infer the existence of human movement based on the standard deviation threshold and these results are presented in Fig. 3.12.

Signal interference due to human motion causes rapid RSSI fluctuations which results in an increased standard deviation. For example, at sample 200, the standard deviation is 4.6280 and at sample 600, the standard deviation is 0.6325. For the dataset shown in Fig. 3.2, we compute the standard deviation of RSSI fluctuation and the computed results are shown in Fig. 3.11.

In addition, more information can be derived from the data, such as, the peak of standard deviation. We infer the existence of human movement based on the standard deviation threshold and present results in Fig. 3.12.

3.5 Optimal Window Size

To study the effect of different window sizes on the detection error rate, we define a sliding window of N samples, where N is a parameter that can be tuned to achieve the desired accuracy for the target environment. The desired value for N would be one that achieves the lowest error detection

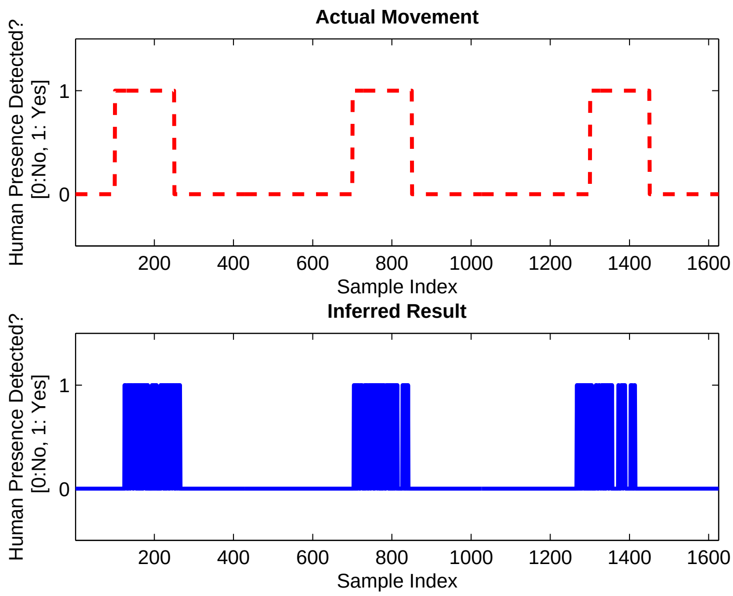

Figure 3.12: Inferred presence of human movement using standard deviation approach

rate, which is calculated by dividing the number of incorrect detections by the total number of samples. We aimed to find an optimal detection window size that minimises the detection error. We studied the accuracy of detection using different sliding window sizes, from $N = 5$ to $N = 100$, across different environments, and also comparing between schemes,

- Overcomplete dictionary approach [4]
- Probability density function approach [5]
- Standard deviation approach [6]

to obtain the results shown in Fig. 3.13.

The detection response time can be shorted by reducing the sliding window size. Let N be the sliding window size and t be the inter-packet interval. The motion can be detected within $N \times t$ seconds, as N samples have to be collected for analysis. Because the inter-packet interval is

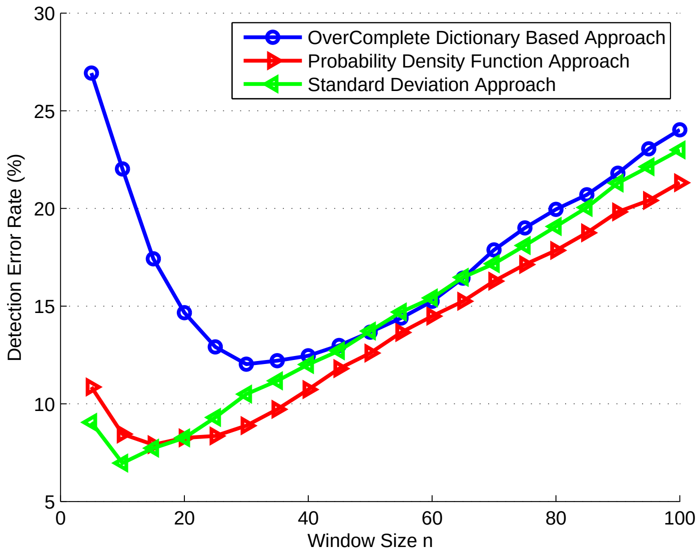

Figure 3.13: Optimal Window Size

consistent throughout the detection, longer detection response time corresponds to larger sliding window size.

3.6 Summary

In this chapter, we first explained and discussed the phenomenon of radio irregularity that is seen as signal strength fluctuation at the receiver end in the presence of human activity. Utilising the received signal fluctuation, we introduced the design of three detection approaches, namely, overcomplete dictionary based pattern recognition (OCPR) approach [4], probability density approach [5] and standard deviation approach [6]. These detection approaches were validated by applying them to the dataset of a small scale detection experiment conducted a 8m $\times$ 6m room. Then, we studied and observed the effect on detection accuracy of the sliding window size and concluded the optimal window size for each detection approach. In the next chapter, we will compare the detection performance of our proposed approaches and the detection approach used in [1].

Chapter 4

Validation of Detection Algorithm

In this chapter, we discuss the experimental validation of the three motion detection algorithms.

In [1], a series of experiments was performed in different locations to evaluate their proposed algorithm. The experiments were conducted in three different meeting rooms of approximate area 6 m $\times$ 4 m. The sensor nodes were placed at a height of 1.5 m and spaced 4 m apart. Over a 20 minute period, a person walked between the sensor nodes every two minutes. RSSI samples were obtained for every received packet. Therefore, the sampling rate is the inter-packet interval of 0.25 sec, so that 100 samples implies a duration of 25 sec. The detection approach used in [1] has resulted in false positives as shown in Fig. 4.1.

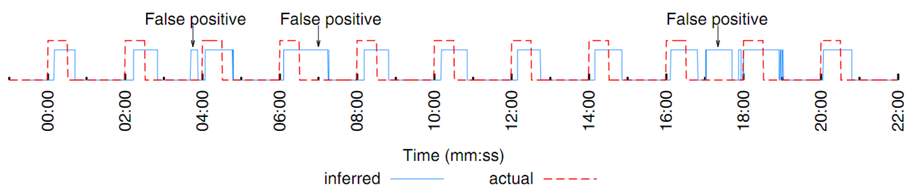

Figure 4.1: False positives by detection method in [1]

4.1 Detection Results

Here, we are not leveraging the RF signals to carry data, which would require accurate synchronization to detect phase, amplitude and/or frequency. However, for the purpose of detection in our work, firstly, we are detecting the relative changes of the signal (i.e. RSSI fluctuations) and we could use the historical signal data or the signal levels immediately before or after for reference; secondly, and more important, we are detecting a pattern out of the reflected signals. As long as the received signals are strong enough, the unstableness of the signals will not adversely affect the performance of our algorithm. The robustness of using RSSI fluctuations (instead of absolute RSSI values) has been experimentally validated by [1]. Therefore the multipath effect will not introduce any unexpected effect to the proposed detection system since the RSSI fluctuation is used.

To explore the performance of different detection approaches, we evaluate and compare the detection accuracy using the dataset acquired in [1]. Two major performance metrics will be considered and discussed in this section. By studying the performance across our proposed detection approaches enable us to exploit the strength and weakness of each approach. Moreover, this study can provides good indication of the suitable usages of each of these approaches.

The two performance metrics are

1. The accuracy of detected movement duration

2. The occurrence of false positive detection

4.1.1 Overcomplete Dictionary Based Approach

The data from [1] was used with the overcomplete dictionary based detection algorithm. We set the window size to $N = 100$ (the same as the window size was used in [1]). The results are shown in Fig. 4.2. The proposed algorithm was able to detect every movement that occurred in the environment, but the accuracy of the movement duration was low.

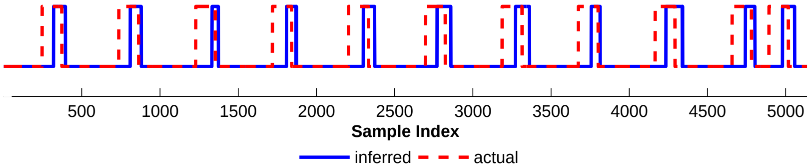

Figure 4.2: Detection results of dataset in [1] by OCPR approach (N=100).

The algorithm was repeated with the window size reduced to $N = 50$ samples. The results given in Fig. 4.3 show that reducing the window size improves the accuracy of both the inferred movement durations and detection latency. Considering that the RSSI fluctuation statistics were gathered for a window of size 100 samples, the pattern of the resulting statistics is not obvious due to this large window size. Non-movement and movement patterns might be mixed over a large window size. For instance, there is a missed detection at sample index of 1300 when N is set to 100 samples. However, the detection result is correct when the window size is reduced to 50 samples. With $N = 100$ samples, the frequency of RSSI fluctuation is calculated with samples from 1201 to 1300 where 1201 to 1229 has non-movement. Therefore, the RSSI fluctuations have a small spike between -1 to 1 as shown in Fig. 4.4(a). This results in an incorrect detection outcome. A smaller window size can improve this performance in both timing and detection duration.

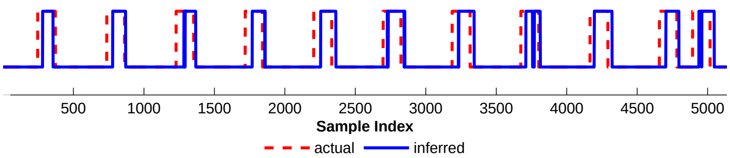

Figure 4.3: Detection results of dataset in [1] by OCPR approach (N=50).

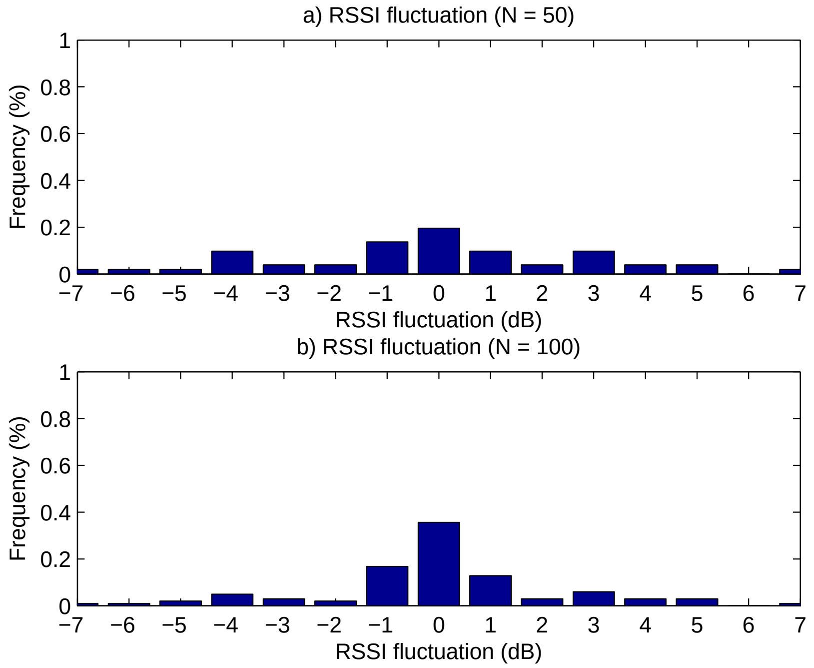

Figure 4.4: RSSI fluctuations (sample index = 1300).

Based on the results shown in Fig. 3.13, we use a sliding window of size $N = 40$ for inferring movement by applying overcomplete dictionary based approach. The optimal inferring result is shown in Fig. 4.5

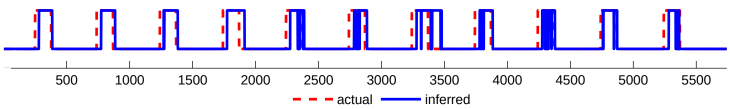

Figure 4.5: Detection results of dataset in [1] by OCPR approach (N=40).

4.1.2 Probability Density Approach

With the same dataset acquired in [1], the probability density approach was applied with sliding window $N = 15$ to obtain optimal inferring results based on results shown in Fig. 3.13. The inferring results are shown in Fig. 4.6. The results shows no false-positive detection with high accuracy of the movement duration.

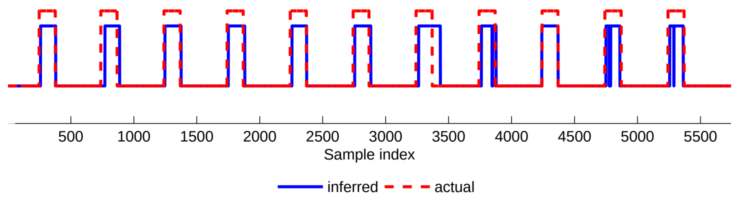

Figure 4.6: Detection results of dataset in [1] by PDF approach(N=15).

4.1.3 Standard Deviation of RSSI Fluctuation Approach

Next we explore the detection performance using the standard deviation approach [6]. The sliding window length is set to 10 and the results are shown in Fig. 4.7. There was no false-positive detection occurred in the results and the accuracy of movement duration was high which indicate the standard deviation was well preformed.

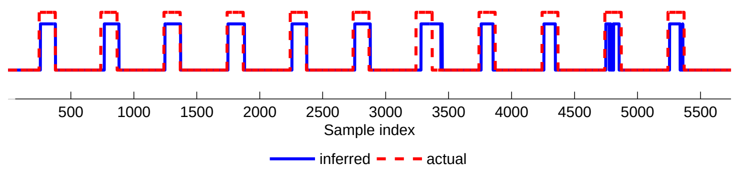

Figure 4.7: Detection results for room 1 by STDEV approach(N=10).

4.1.4 Performance Comparison

The summary of the performance of our proposed detection approaches is presented in table 4.1. The inferring results of our proposed approaches show no occurrence of false-positive detection with high accuracy of detected movement duration. However, by comparing the window size, it is obvious that the probability density function approach and standard deviation approach outperform the overcompelete dictionary based approach since smaller window size was required to achieve optimal detection accuracy. Smaller window size implies the quicker detection response which is essential for some detection systems. In addition, the standard deviation approach provides statistical information from the data, such as, the peak of standard deviation.

Detection Approach	Sliding Window Size	Accuracy Duration of detected movement	False-Positive
Overcomplete Dictionary Based Approach	**40**	**High**	**No**
PDF Approach	**15**	**High**	**No**
Standard Deviation Approach	**10**	**High**	**No**

Table 4.1: Comparison between proposed approaches

4.2 Summary

In this chapter, we first compared the detection performance of our proposed detection approaches with the one used in [1]. Two performance metrics were considered (the accuracy of detection duration and the occurrence of false-positives). With the data from [1], the occurrence of false-positive detection is eliminated with high accuracy of detection duration using the proposed detection approaches. While high detection accuracy is achieved, we then studied the most suitable detection approach for automated people counting systems. The standard deviation approach is considered the most suitable detection approach for automated systems due to it not only achieves high accuracy detection but also provides statistical information from the data. In next chapter, we will briefly discuss the wireless sensor node that we used in our larger scale experiments and then studied on the characteristic of RF signals.

Chapter 5

Testbed Setup

Larger scale experiments are conducted to demonstrate how the detection algorithms can be used for people counting. Here, we first describe the hardware specification of two key devices used in our experiments, namely, the sensor nodes manufactured by Texas Instruments MSP430 [25] and Lebelium Waspmote [26]. Then, we perform and discuss preliminary studies on their RF characteristic in order to achieve optimal detection performance.

5.1 Wireless sensor node specification

Various types of wireless sensor node are used in different type of WSN applications to fit specific needs. There were two types of wireless sensor node used in a series of experiments that are presented in this thesis. We will briefly discuss the hardware specifications of the wireless sensor nodes in this section.

5.1.1 Texas Instrument MSP430-CC2500

Texas Instruments (TI) provides a platform called the MSP430 wireless development tool [25]. The core of this development board is the MSP430 microcontrollers. This microcontroller is made by Texas Instruments and there is a complete family of MSP430 microcontroller. The communicating unit of this development board is a CC2500 2.4 GHz, ISM band multi-channel RF transceiver which uses SimpliciTI as its network protocol [27]. SimpliciTI provides an API for packet transmission between an Access Point and End Devices. The Access Point is USB-powered and connected to computer. The End Device is powered by an AAA battery which enables easy deployment. The RF transceiver provides a transmission range for only 8 meters due to the use of a chip antenna. In addition, the transmission range largely depends on the physical environment and the usage of the RF channel. MSP430 wireless development board was used in the preliminary studies on RF characteristics which will be discussed in Section 5.2.

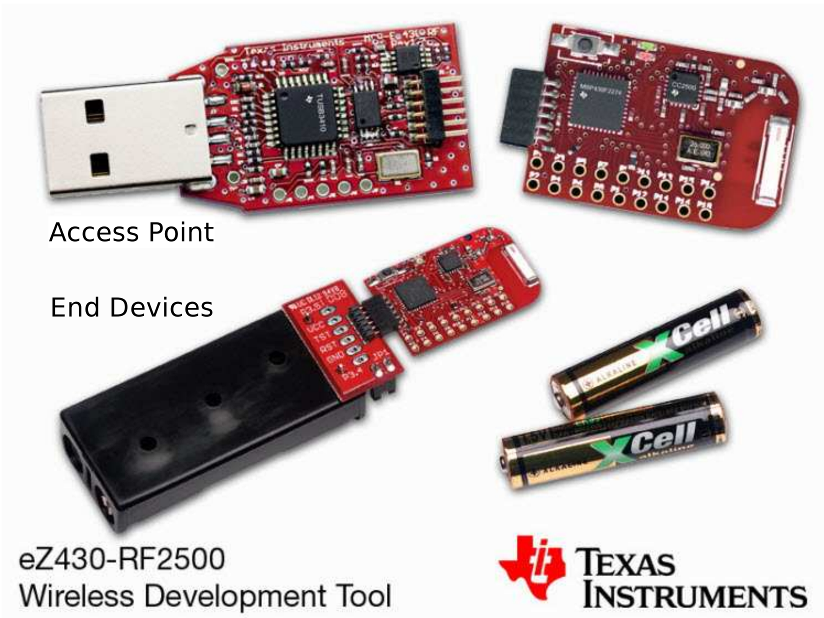

Figure 5.1: Texas Instrument MSP430-CC2500

5.1.2 Lebelium Waspmote

Waspmote [26] was designed by Lebelium in 2009 and is used for both research and commercial purposes. Waspmote is an open source electronic prototyping platform based on the Arduino [28] extended with Waspmote's libraries. The Waspmote board was deployed in our larger-scale experiments due to its advantage of long transmission range. The Waspmote board comes with a ATmega1281 processor and various communication modules can be used such as ZigBee, Bluetooth, GSM/GPRS, and IEEE 802.15.4. The IEEE 802.15.4 communication module with 2 dBi dipole antenna was used in our experiment. The ideal transmission range is 500 m with 1 mW transmission power.

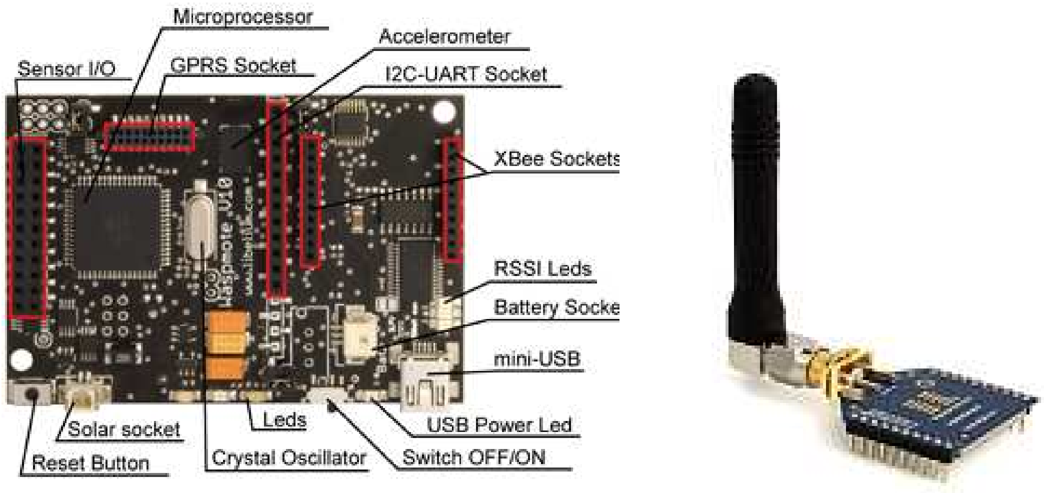

(a) Lebelium Waspmote [26]

(b) XBEE IEEE802.15.4 module

Figure 5.2: Hardware Specification of Waspmote and XBee module

5.2 Preliminary Studies of RF Characteristics

In order to achieve optimal detection performance, the preliminary studies on the various effects on radio irregularity are essential. These effects are such inter-packet interval, transmission power and frequency channel. Based on these studies, the optimal configuration can be deduced and used in later experiments.

5.2.1 Inter-packet Interval

The Inter-packet interval is the transmission interval between successive packets. The receive signal strength is recorded on reception of the packet. Hence, the precision of inferring movement is higher with shorter of inter-packet interval. However, the power consumption is the major drawback of shorten the inter-packet interval for the battery powered devices such as wireless sensor nodes. In addition, the limited computation power of sensor nodes could be a bottleneck when a short inter-packet interval is used.

The performance of detection could be largely depending on the inter-packet interval. Ther effect was investigated and the results are shown in 5.1

	Detection Approach		
Interval	1	2	3
0.1 s	2.33%	2.56%	1%
0.15 s	1.7%	7.3%	3%
0.20 s	27.3%	9.1%	6.3%

Table 5.1: Detection Error Rate against Inter-Packet Interval

For the results above, we observe the lowest detection error rate is obtained when the inter-packet interval is shortest using probability density function approach [5] and standard deviation approach [6]. As the inter-

[1]Overcomplete Dictionary Based Approach
[2]Probability Density Approach
[3]Standard Deviation of RSSI Fluctuation Approach

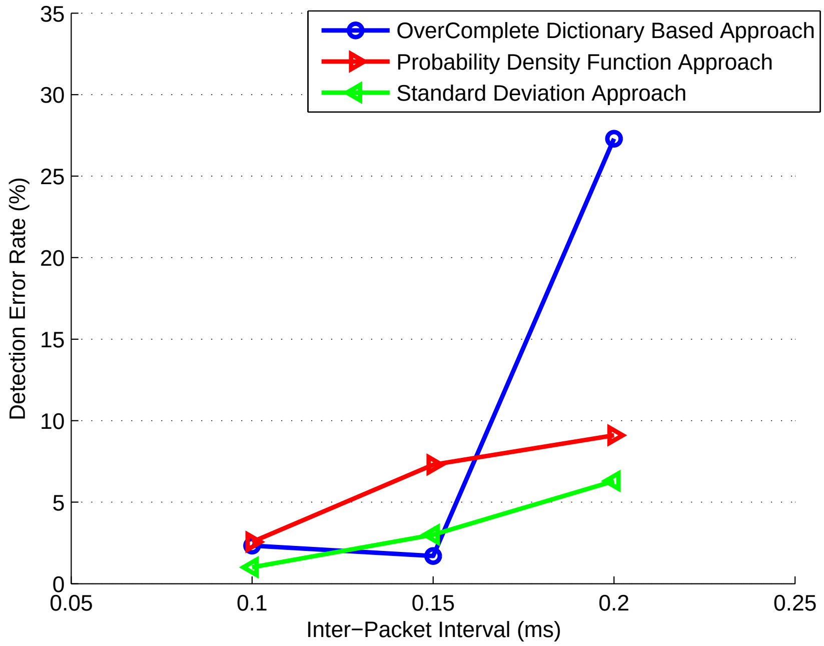

Figure 5.3: Detection Error Rate against Inter-Packet Interval

packet interval increases, a higher detection error rate is observed. The detection response time largely depends on the combination of sliding window size and the inter-packet interval which is discussed in the previous chapter.

5.2.2 Transmission Power

In wireless communication, the transmission power plays a crucial role in ensuring the transmitted packet can be received by receivers. Radio-frequency signals can be degraded by interference by several components such as other wireless equipment, materials, and moving objects blocking the line-of-sight transmission path. With stronger transmission power, the bit error rate of packet transmission is lower due to a higher signal noise ratio(SNR) at the receiver.

Transmission power could be as another major determinant for detection accuracy in our detection system. Therefore, a series of experiments was conducted to observe the accuracy of detection using different transmission power, from -4 to 1 dBm and also comparing between detection schemes, namely, the overcomplete dictionary approach [4], probability density function approach [5] and standard deviation of RSSI fluctuation approach [6]. The results are shown in Table 5.2 and Fig. 5.4.

	Detection Approach		
Tx Power	1	2	3
-4 dBm	27.4194%	9.1129%	8.8710%
0 dBm	28.5484%	11.0484%	9.8387%
1 dBm	27.500%	14.7581%	12.3387%

Table 5.2: Detection Error Rate against Tx Power

The detection error rate ranges from 9.11% to 14.76% and 8.87% to 12.34% for the standard deviation approach [6] and theprobability density function approach [5], respectively. However, the overcomplete dictionary based approach [4] was not performing well with the overall error rate ranging from 27.42% to 28.55%. The accuracy of detection varies by 5% range across different transmission power for the same detection scheme. The variance of detection error rate for the same detection approach is minor. Hence, the influence on detection accuracy of different transmission power is minimal.

5.2.3 Wireless Channel Frequency

In our experiment, the IEEE 802.15.4 communication module was used for wireless sensor nodes. The physical radio frequency transceiver operates in the industrial, scientific and medical (ISM) radio bands. The ISM

[1] Overcomplete Dictionary Based Approach
[2] Probability Density Approach
[3] Standard Deviation of RSSI Fluctuation Approach

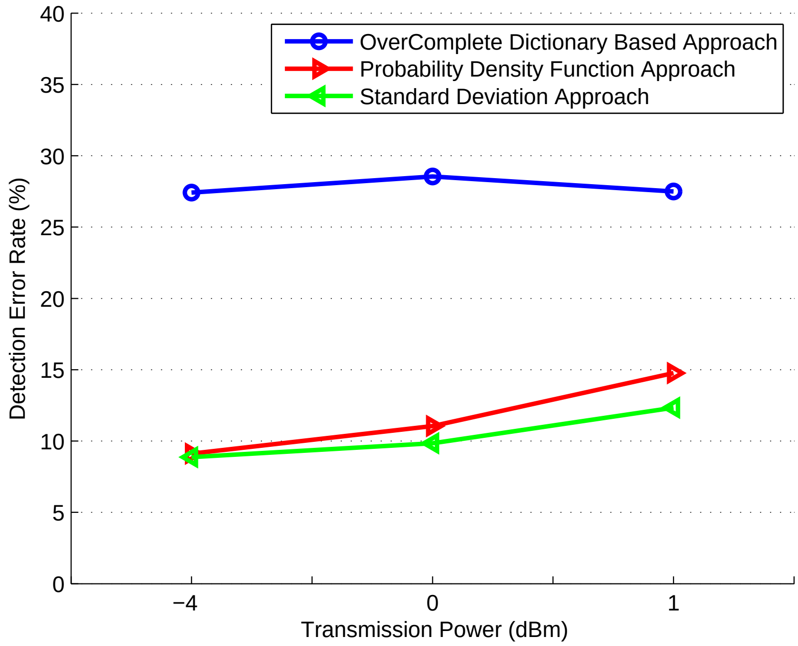

Figure 5.4: Detection Error Rate against Tx Power

band is designed for the use of radio frequency energy for industrial, scientific and medical purposes. The most commonly known ISM device is the home microwave oven which operates at 2.45 GHz with high power. In recent years, the ISM band has also been shared with communication applications such as wireless sensor networks, wireless LANs and cordless phones. All these communication devices can be interfered with each other up to a certain degree depends on the level of transmission power is used. The radio spectrum of ISM band ranges from 2400-2483.5 MHz.

We conducted a series of experiments to observe and study the behaviour of detection accuracy with respect to different radio frequencies by varying the frequency from 2433 MHz to 2481 MHz with fixed transmission power and inter-packet interval. We applied different detection schemes to compare the detection error rate. The results are shown in Table 5.3 and Fig. 5.5.

	Detection Approach		
Frequency	1	2	3
2433 MHz	28.3484%	9.696%	10.682%
2451 MHz	27.4194%	9.1129%	8.871%
2457 MHz	25.8723%	6.0426%	6.0426%
2463 MHz	26.0341%	7.1371%	6.6504%
2481 MHz	29.9592%	13.7959%	12.4898%

Table 5.3: Detection Error Rate against Wireless Channel

The detection error rate is relatively consistent using the same detection scheme across the various radio frequency. A lower detection error rate is observed with radio frequency at 2457 MHz. This could be due to the channel being relative cleaner than other frequency. By cleaner, we mean the channel is less used by other communication devices.

As we recall the major components that can interfere with the RF signal, namely, the interference of other wireless devices and materials, are consistent and stable throughout the experiment. On the other hand, the line-of-sight blocking by the moving object has significant interference compared to other interference components.

5.3 Summary

In this chapter, we started with discussing the hardware specification of two types of sensor nodes that were used in our experiments. In preliminary studies on RF characteristics, we discussed the various effects of RF signals that are affecting the detection performance. We observed the detection error rate is lower and the detection response time quicker with

[1] Overcomplete Dictionary Based Approach
[2] Probability Density Approach
[3] Standard Deviation of RSSI Fluctuation Approach

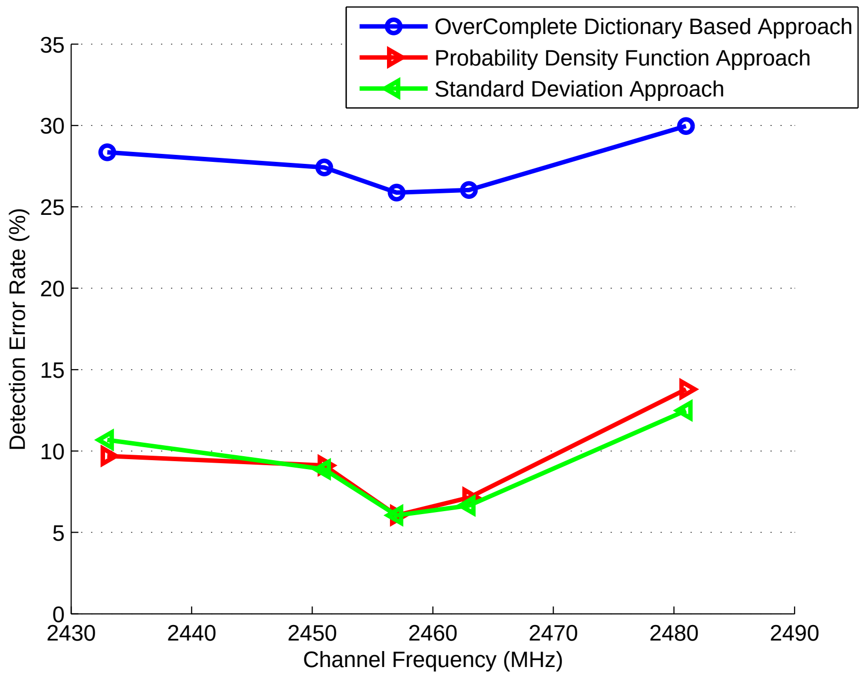

Figure 5.5: Detection Error Rate against Wireless Channel

short inter-packet interval. Next, we found that the effect of transmission power on detection error rate is insignificant. Finally, the detection error rate is consistent across the various radio frequency. We will discussed the design of automated people counting system in the next chapter.

Chapter 6

Automated People Counting

Accurate detection of human movement is just the initial step to achieving the goal of automated people counting. The next step is the ability to infer that more than one person has crossed the area of interest.

In this chapter, we first introduce the conceptual sensor configuration and discuss the design of a people counting system using the configuration of a single transmitter and multiple receivers to differentiate the number of passers by. Then, we discuss the use of discriminant analysis to achieve the classification of number of passerbys in controlled and uncontrolled environments.

6.1 Single transmitter-single receiver

First, a series of experiments were conducted to observe the precision of the detection algorithm in a realistic indoor environment, namely, a corridor in a university building, as shown in Fig. 6.1, where the two red dots indicated by the arrows refer to the transmitter/receiver pair using IEEE802.15.4 technology. The devices are spaced 1.5m apart (width of corridor) and placed at a height of 1.1m, on a ledge. Each data collection duration was 300 seconds with inter-packet interval time of 0.15 seconds, during which the number of people who have walked past the devices were recorded and tagged with the time. Fig. 6.2 shows the results for one data collection period, during which nine persons walked through individually and two pairs of people past while walking close to each other, at the sample index of 484 and 925. In the detection results, shown in Fig. 6.2, a total of 11 movements were detected. It is clear that detecting two people walking side by side is a major challenge as the RSSI fluctuations arising from one and two persons passing are quite indistinguishable.

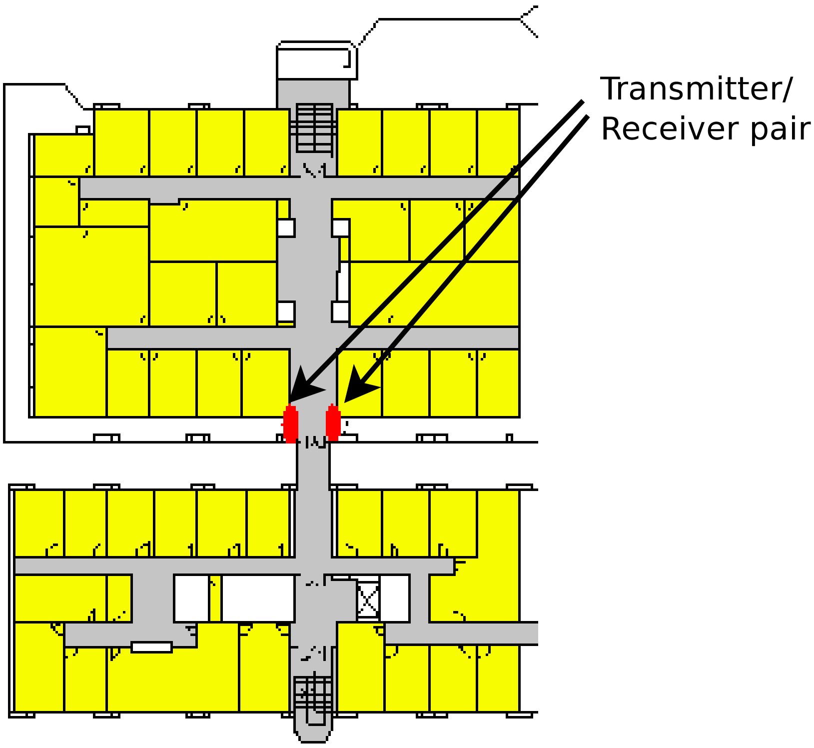

Figure 6.1: Deployment along corridor of building in university

6.2 Single transmitter-multiple receiver

In a pervasive network environment, it is not inconceivable to have numerous small wireless devices present. A conceptual deployment scenario

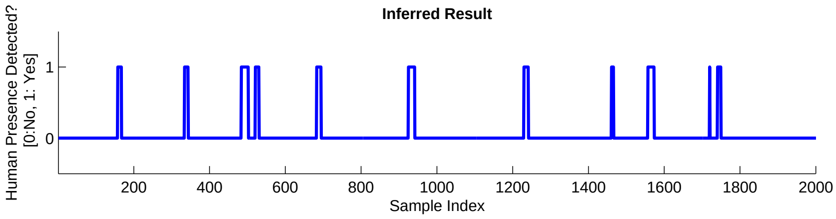

Figure 6.2: Detection of pedestrian traffic along corridor

like that shown in Fig. 6.3 can be assumed, and we look at a subset configuration of one-transmitter and two-receivers as shown in Fig. 6.4.

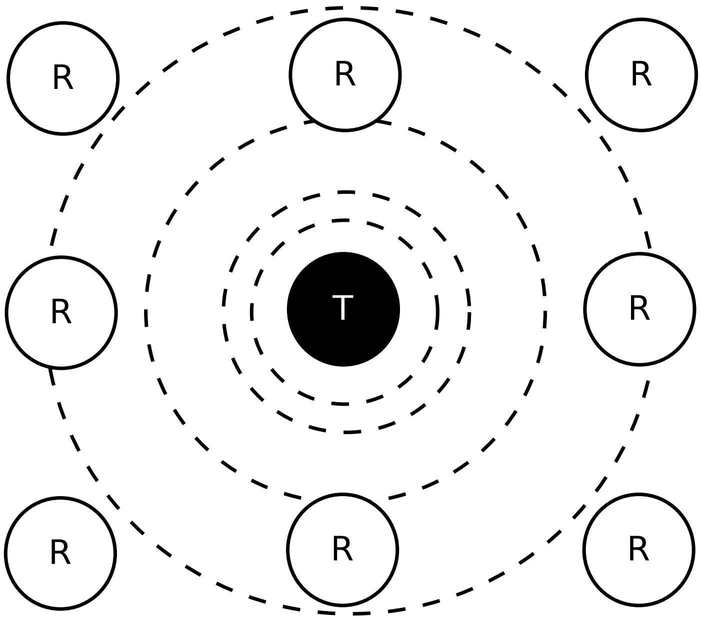

Figure 6.3: Conceptual Configuration

Using the one-transmitter two-receiver configuration, the transmitter broadcasts packets at a rate of one packet every 0.15 seconds. Receiver R_1 is 1.5m from transmitter T (d_1 = 1.5m)and R_2 is 1.5m from R_1(d_2 = 1.5m). As two persons walk along the path between T and the two receivers in the direction shown in Fig. 6.4, they first cross the T-R_2 signal transmission path, followed by the T-R_1 signal path. A key point to note is the different signal interference zones that result from the movement of the

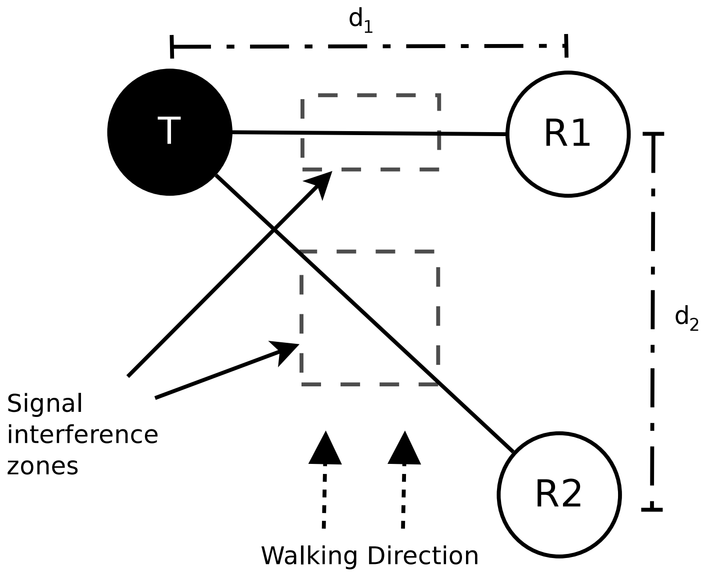

Figure 6.4: One-Transmitter Two-Receiver Configuration

two persons.

First, we collected data for one person walking across the signal transmission path (passing first R_2 then R_1) to be used as the reference case. The detection results correctly show that one person passed at around the time of sample 100 and another at around sample 200, as shown in Fig. 6.5. Intuitively, the detection result at sample 100 is more logical since the person passed R_2 first, then R_1. However, as the two receivers are very close to each other, having the two receivers showing signal fluctuations at almost the same instant is also likely, especially when the person is walking fast.

Next, we collected data for the case of two persons walking side-by-side in the direction of R_2 to R_1 as shown in Fig. 6.4. We expect that the detection duration of T-R_2 should be longer than T-R_1. This is because the T-R_2 signal experienced a longer duration of interference than the T-R_1 signal. The detection result of two people walking from R_2 to R_1 shown in Fig. 6.6 confirms our hypothesis. However, we also observed a false positive detection at sample 64. As the two receivers are placed closed to each other, 1.5m apart, we can assume that it is unlikely for a moving object to be detected by one receiver but not the other. Therefore, we can remove such false positive detections by comparing and matching the data from both receivers and to achieve the desired results as shown in Fig. 6.7.

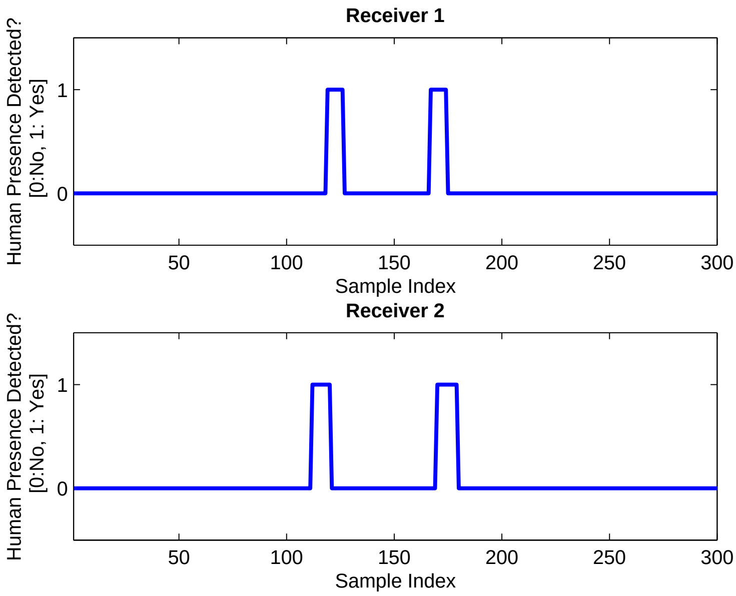

Figure 6.5: One person walking in the direction of R2 to R1

6.3 Controlled Environment Setup

In order to exploit the effect of RSSI fluctuation caused by signal interference by a few people, we conducted a series of experiments with a variable group size (ranging from one to five people) under a controlled indoor environment. Sensor motes using IEEE802.15.4 wireless technology were deployed in a 6m×8m room in a one-transmitter two-receiver configuration (Fig. 6.4.) The motes were placed at a height of 0.9m. Receiver R_1 was placed 3.5m from transmitter T (d_1 = 3.5m) and R_2 at 2m from R_1(d_2 = 2m). The transmitter, T, broadcasts packets continuously in time intervals

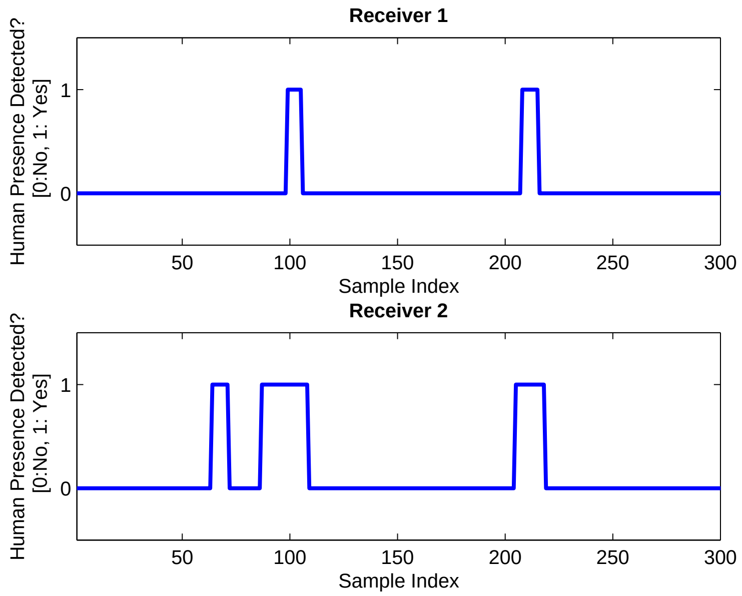

Figure 6.6: Two people walking in the direction of R2 to R1

of 0.15s. The absolute RSSI values were recorded upon packet reception at the receivers. Then, groups comprising one to five people made five consecutive round trips between the transmitter and two receivers. Five experiments were conducted for each group. The formation of test subjects is aligned in a single row and moving at the same speed passing between transmitter and receivers. Stronger interference of radio signals is expected from larger mass as the number of people increases. In addition, the difference of interference duration could also be significant.

In our experiments, we assume that the pedestrians are walking side by side in both directions. Since only the level of interference and duration of positive detection is considered, the direction of movement will not impact on our proposed counting system. Due to the quick response detection time, different groups of people can be distinguished and treated individually. For example, our proposed detection system is able to detect two groups of two persons if they walk past transmitter-receiver pairs along the corridor within the minimum response time, which is determined by

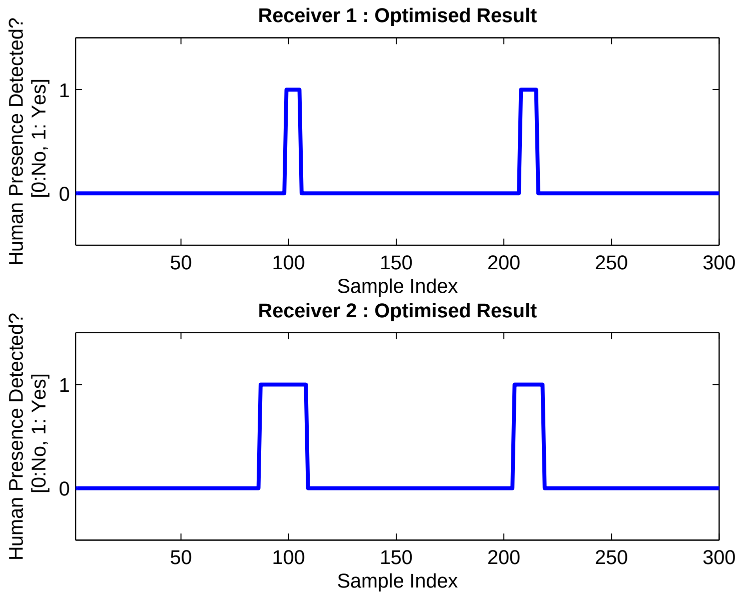

Figure 6.7: Optimised Result of multiple receivers

the sliding window size and the inter-packet interval used. The detection response time can be shortened by reducing the sliding window size. If we let n denote the sliding window size and t denote the inter-packet interval (measured in ms), then the motion can be detected within $n \times t$ ms since n samples have to be collected before analysing and determining the motion.

6.4 Data Analysis

We use *discriminant analysis*, a method to find the linear combination of measurements which characterize two or more groups [29], to analyze the collected data. The key concept of the *discriminant analysis* approach is to classify the number of people based on the difference in the influence on RSSI readings if the size of the interference zone.

6.4.1 Discriminant Analysis

This is a method widely used in statistics, pattern recognition and machine learning because of its ability to characterize two or more classes. Discriminant Analysis attempts to express one dependent variable, in our case the number of pedestrian, as a linear combination of other independent variables such as measurements of RSSI readings.

We let a finite number g denote the distinct number of groups which in our case is five (i.e. g=5, denoting groups of 1–5 persons). We refer to the G_i as groups where $i = 1, \dots, 5$. There are two phases of discriminant analysis which are *training* and *classification*. The system identifies differences in RSSI fluctuations caused by different number of people as signatures in the training phase. It is important to note that this training is only required once to identify the fluctuations caused by differing numbers of people, and not for each deployment scenario. During the training phase, a total of $g - 1$ orthogonal discriminant functions are constructed such that the groups differ as much as possible on discriminant score D. The form of the linear discriminant function is:

$$D = v_1 X_1 + v_2 X_2 + ... + v_i X_i + c \tag{6.1}$$

where

$$\begin{aligned} D &= \text{discriminant score} \\ v &= \text{the discriminant coefficient} \\ X &= \text{the value of each independent variable} \\ c &= \text{a constant} \\ i &= \text{the number of independent variables} \end{aligned}$$

Once the discriminant functions are constructed, the discriminant analysis enters the second phase which is classification. Fisher's linear discriminant analysis [30] is used for data classification; the purpose of Fisher's technique is to find the line of projection that separates different groups [31].

6.5 Training Phase of Discriminant Analysis

We use the standard deviation of RSSI fluctuations of detected movement as the primary dataset. For instance, the standard deviation of RSSI fluctuations of one of the experiments for one person is shown in Fig. 6.8.

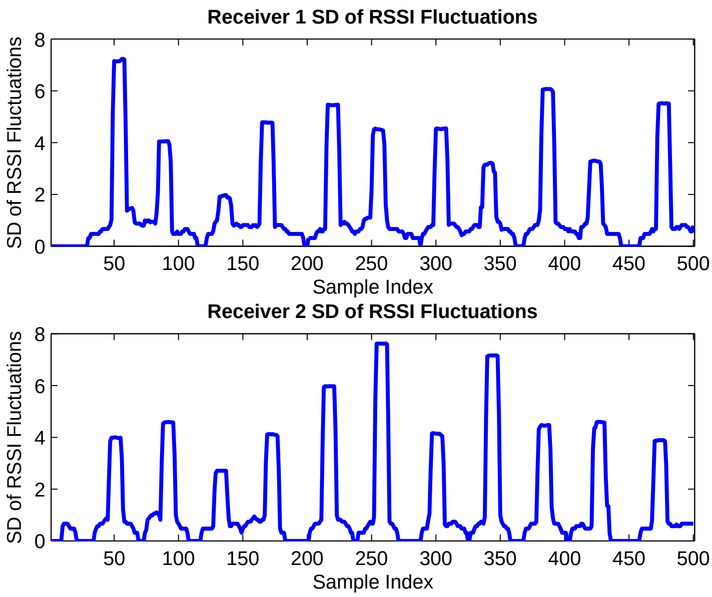

Figure 6.8: Experimental Data for one person in a single experiment

We utilize the information from each positive detection, particularly mean, standard deviation (std), coefficient of variation (CV), detection duration and area under the curve, to be the independent variables in order to achieve high discrimination between groups. The more statistical information we can extract from these positive detections, the greater the ability to discriminate between the different size groups.

The methods to extract the statistical information are described below.

- **Mean** is calculated as the sum of the standard deviations of RSSI fluctuation greater than a detection threshold, and the total number of positive detection.

- **Standard deviation** of the positive detection is taking the standard deviation of RSSI fluctuations that are above the detection threshold.
- **Coefficient of variation** is defined as the ratio of the standard deviation to the mean which is the calculated standard deviation divided by the mean.
- **Duration** is the number of samples that have the standard deviation of RSSI fluctuations greater than the detection threshold.
- **Area under the curve** is calculated by the duration times the sum of the standard deviation of RSSI fluctuation.

We use the SPSS [7] software to perform discriminant analysis. For a total of 50 samples of each group, the mean of each independent variable is plotted in Fig. 6.9. The duration and area under the curve are the two most significant independent variables. The detection duration of R_1 is stable throughout all groups while the detection duration of R_2 steadily increases as the number of people increase. This trend is as expected since more time is needed to pass the T-R_2 transmission path than T-R_1. The area under the curve follows the same trends as longer detection duration makes the area under the curve larger.

Next, these independent variables are taken to construct the discriminant functions that maximize the separation between each group. In Table 6.1, it provides very high F values and lower Wilks' Lambda as evidence of significant difference in R_2 detection duration than any other independent variables. In addition, in statistical significance testing, the null hypothesis is rejected when the p-value is smaller than the significance level α which is 0.05. The results are considered to be statistically significant when null hypothesis is rejected.

The information of each discriminant function is shown in Table 6.2. There are five groups, namely 'one person' to 'five people' and as a result four discriminant functions are produced. With high Eigenvalue and percentage of variance, function 1 covers most total statistical population.

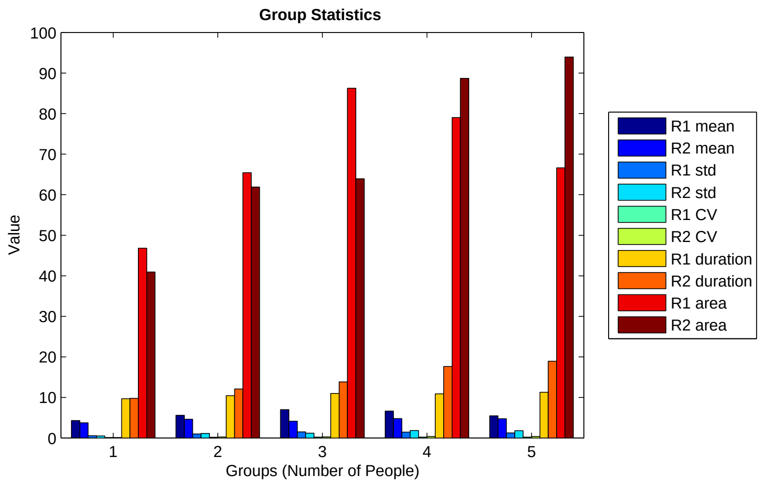

Figure 6.9: Mean of independent variables of each group

The relative importance of each independent variable in each discriminant function can be found by analyzing the structure matrix table. These 'Pearson' coefficients are discriminant loadings which act like factor loadings in factor analysis [32]. Generally, an absolute value of 0.3 is taken to be the threshold that separates a significant from an unsignificant variable. For example, we have five independent variables in discriminant function D_1, namely, 'R_1 CV', 'R_2 CV', 'R_1 duration', 'R_2 duration', and 'R_2 area' that discriminates between groups.

The discriminant function coefficient shows the contribution of each independent variable to the discriminant function. It operates like a regression equation. For example, the discriminant function D_1 and D_2 are shown below.

$$\begin{aligned} D_1 = &(0.26 \times R_1 mean) + (-0.837 \times R_2 mean) + \\ &(-1.033 \times R_1 std) + (0.999 \times R_2 std) + \\ &(17.142 \times R_1 CV) + (3.964 \times R_2 CV) + \\ &(0.298 \times R_1 duration) + (0.306 \times R_2 duration) + \\ &(0.011 \times R_1 area) + (0.002 \times R_2 area) - 10.805 \end{aligned} \tag{6.2}$$

IV	Wilks' Lambda	F	p-value
R_1 mean	0.773	17.986	0.001
R_2 mean	0.992	5.207	0.000
R_1 std	0.640	34.437	0.000
R_2 std	0.692	27.311	0.000
R_1 CV	0.485	65.034	0.000
R_2 CV	0.436	79.137	0.000
R_1 duration	0.633	35.572	0.000
R_2 duration	0.256	178.008	0.000
R_1 area	0.713	24.605	0.000
R_2 area	0.603	40.256	0.000

Table 6.1: Test of Equaltiy of Group Means

Functions	Eigenvalue	% of variance	Canonical Correlation
1	5.717	82.9	0.923
2	0.952	13.8	0.698
3	0.146	2.1	0.357
4	0.084	1.2	0.279

Table 6.2: Table of Eigenvalues

$$\begin{aligned} D_2 = &(0.863 \times R_1 mean) + (-1.044 \times R_2 mean) + \\ &(-1.023 \times R_1 std) + (1.046 \times R_2 std) + \\ &(17.026 \times R_1 CV) + (-6.788 \times R_2 CV) + \\ &(0.225 \times R_1 duration) + (-0.203 \times R_2 duration) + \\ &(0.017 \times R_1 area) + (-0.003 \times R_2 area) - 2.414 \end{aligned} \tag{6.3}$$

Fig. 6.10 plots for all samples of discriminant functions 1 and 2 which cover 96.7% of variance. The group centroids are plotted from left to right as the number of people increase. This is a good indication that the groups

	Function			
	1	2	3	4
R_1 mean	0.153	0.384	-0.047	0.477
R_2 mean	0.094	-0.088	0.243	0.464
R_1 std	0.275	0.361	-0.051	0.235
R_2 std	0.269	-0.109	0.049	0.486
R_1 CV	0.417	0.219	0.387	-0.162
R_2 CV	0.468	-0.093	0.070	0.603
R_1 duration	0.306	0.111	0.417	-0.296
R_2 duration	0.692	-0.411	-0.206	-0.098
R_1 area	0.191	0.438	0.020	0.372
R_2 area	0.326	-0.212	0.094	0.288

Table 6.3: Structure Matrix

are well discriminated by functions D_1 and D_2.

Finally, the classification is performed based on the discriminant score. The classification results are shown in Table 6.5. All perfect prediction cases lie on the diagonal. The classification results show 81.6% overall accuracy in detecting the number of people comprising a given group. Further, an overall accuracy of 97.9% was achieved in predicting individual head counts. For example, the actual head count of 250 samples is 750 and the predicted head count was 734.

6.6 Uncontrolled Environment Setup

In order to evaluate the accuracy in counting the number of people with no specific formation using the discriminant function that is calculated in the previous section, we deployed the wireless sensor nodes in an uncontrolled environment. We deployed a configuration of one transmitter and

	Function			
	1	2	3	4
R_1 mean	0.260	0.863	0.611	0.084
R_2 mean	-0.837	-1.044	0.843	0.460
R_1 std	-1.033	-1.023	-4.612	-0.471
R_2 std	0.999	1.046	-1.165	-0.934
R_1 CV	17.142	17.026	32.236	-12.682
R_2 CV	3.964	-6.788	2.522	12.729
R_1 duration	0.298	0.225	0.514	-0.358
R_2 duration	0.306	-0.203	-0.140	-0.146
R_1 area	0.011	0.017	-0.001	0.018
R_2 area	0.002	-0.003	0.005	0.012
(Constant)	-10.805	-2.414	-10.974	2.054

Table 6.4: Canonical Discriminant Function Coefficient

three receivers, as shown in Fig. 6.11a where the darker areas represent corridors and walkways. Three receivers were placed on one side of a wide corridor with one transmitter on the opposite side. The distance of T-R2 is 3m which allows up to five people walking past the corridor side-by-side. The distance of R1-R2 is 2.5m is the same as the distance of R2-R3. This sensor placement configuration can be considered as two sets of one-transmitter two-receiver configuration in symmetry. Each experiment was conducted for 15 minutes. The total number of people walking past was recorded on video to compare for verification of the detection result. A video frame of an experiment in progress is shown in Fig.6.11b.

For convenience in data analysis and comparison, the data collection was separated into 3-minute periods. Fig. 6.12 shows the results for one data collection period, during which our proposed detection system has been able to correctly infer every single occurrence of passerbys crossing the sensing zone. The recorded video shows the sequence of people in

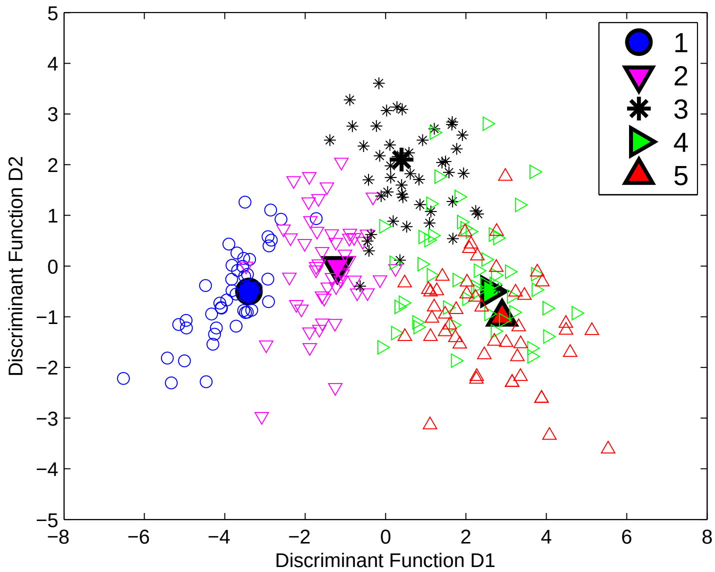

Figure 6.10: Combined Group Plots of Discriminant Function 1 and 2

groups walking past the corridor as {2, 1, 1, 3, 1, 1, 1, 1, 3, 1}. The detection duration difference between receivers increases for 1st, 4th and 9th positive detections. As discussed previously, this is caused by the larger interference zone when more than one person passes, as shown in Fig. 6.4.

Using the one-transmitter three-receiver configuration, two sets of statistical information relating to positive detections can be extracted since it contains two sets of one-transmitter two-receiver configuration. When applying new cases, the discriminant score will be calculated using the discriminant functions that are constructed during training phase. All new samples' discriminant scores of discriminant 'Function 1' and 'Function 2' for R1-R2 and R3-R2 are plotted in Fig. 6.13 and Fig. 6.14 respectively. A sample can be classified when its discriminant score lies on the diagonal to the group centroid which is shown as a filled marker.

We select a sample of the experiments for discussion, where a total of 90 people walked past the sensing zone in groups ranging from one to five

	NPeople	Predicted Group Membership					
		1	2	3	4	5	Total
Count	1	47	3	0	0	0	50
	2	3	46	1	0	0	50
	3	0	3	44	2	1	50
	4	0	3	7	31	9	50
	5	0	0	0	14	36	50
%	1	94	6	0	0	0	100
	2	6	92	2	0	0	100
	3	0	6	88	4	2	100
	4	0	12	14	62	18	100
	5	0	0	0	28	72	100

Table 6.5: Cassification Results

persons.

We select a sample of the experiments for discussion, where a total of 39 people walked past the sensing zone in groups ranging from one to three persons; as this was an uncontrolled environment, we had not been able to detect groups of larger sizes although some of the instances could have been classified as a larger group.

First, we present the classification results for R1-R2 which are summarized in Table 6.6 . From the R1-R2 dataset, the accuracy of predicting the number of people comprising a given group is 76%, which is slightly lower than that for the controlled environment. This is expected as a few people walking in close proximity can be grouped in different ways from different angles and their relative positions with the group can change dynamically. More importantly, we aim to estimate the number of people in total, and that we have been able to achieve with an accuracy of around 94.4% for this experiment, and with similar accuracies for other experiments. This is very close to the accuracy achieved in the controlled environment.

	NPeople	Detected Group Membership					
		1	2	3	4	5	Total
Count	1	**26**	2	2	0	0	30
	2	1	**6**	2	0	0	9
	3	1	1	**3**	0	0	5
	4	0	0	0	**2**	1	3
	5	0	0	0	0	**3**	3
%	1	**86.7**	6.67	6.67	0	0	100
	2	11.1	**66.7**	22.2	0	0	100
	3	20	20	**60**	0	0	100
	4	0	0	0	**66.7**	33.3	100
	5	0	0	0	0	**100**	100

Table 6.6: R1-R2 Prediction Results under Uncontrolled Environment

Next, we present the data from R3-R2, tabulated in Table 6.7. The accuracy of group size estimation dropped to 57.8% for the same reasons as the R1-R2 case. The accuracy for number of people detected is 84.4% with a noticeable degree of over-counting. Upon careful analysis of the video, we identified a possible cause of the over-counting that led to the higher estimation error. From Fig. 6.11a, we note that R3 is located next to a stairwell on the left. That is a highly utilized staircase and, as a result, many people pass close to R3 but not necessarily continue right along the corridor across the R3-R2 sensing zone. This has resulted in two instances of over-estimating the group size by more than one, where a group of two people has been detected as a group of four people. E.g., if a group four people come down the stairs and split into two groups of two, with one group continuing right along the corridor across the R3-R2 sensing zone while the other, moving in the opposite direction or straight across to the walkway on the lower left of Fig. 6.11a, then there is a higher probability of the group size prediction being affected.

	NPeople	Detected Group Membership					
2		1	2	3	4	5	Total
Count	1	**22**	5	3	0	0	30
	2	1	**5**	1	2	0	9
	3	0	1	**3**	1	0	5
	4	0	0	1	**1**	1	3
	5	0	0	0	1	**2**	3
%	1	**73.3**	16.7	13.3	0	0	100
	2	11.1	**55.6**	11.1	22.2	0	100
	3	0	20	**60**	20	0	100
	4	0	0	33.3	**33.3**	33.3	100
	5	0	0	0	33.3	**66.6**	100

Table 6.7: R3-R2 Prediction Results under Uncontrolled Environment

Based on the assumption that we intend to utilize pre-deployed wireless communication devices, the R3-R2 case highlights the need for careful selection of transmitter-receiver combinations in order to minimize detection errors. For the R1-R2 case, although R1 is also near the building entrance/exit on the right, its position is sufficiently far away such that people moving in and out of the entrance/exit will not have a significant effect, on its detection.

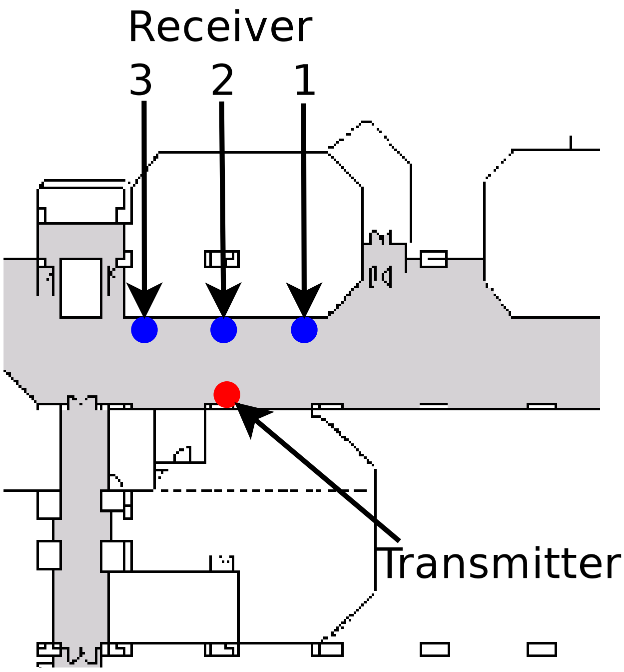

(a) Layout of Sensing Zone

(b) Experiment in progress with passerbys crossing

Figure 6.11: Test Environment

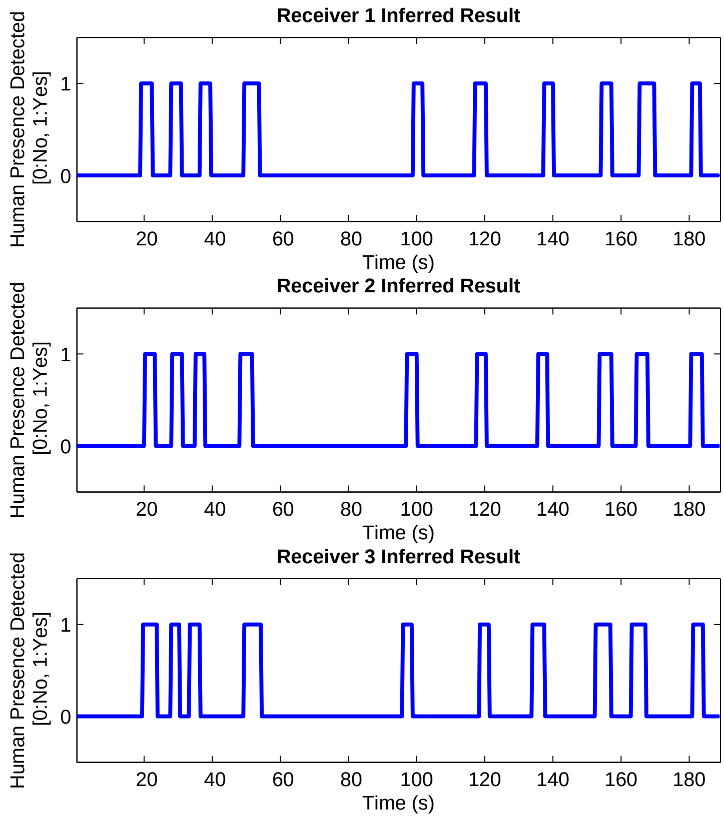

Figure 6.12: Inferring Results under Uncontrolled Environment

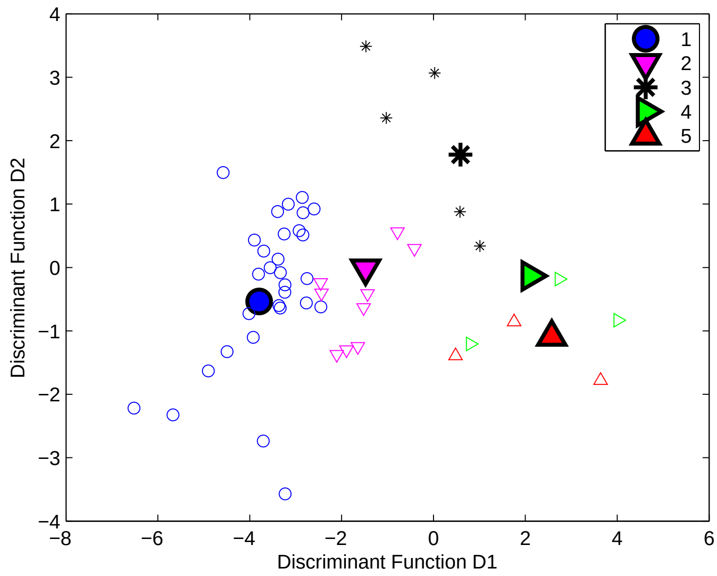

Figure 6.13: Combined Group Plots of Discriminant Functions 1 & 2 for R1-R2

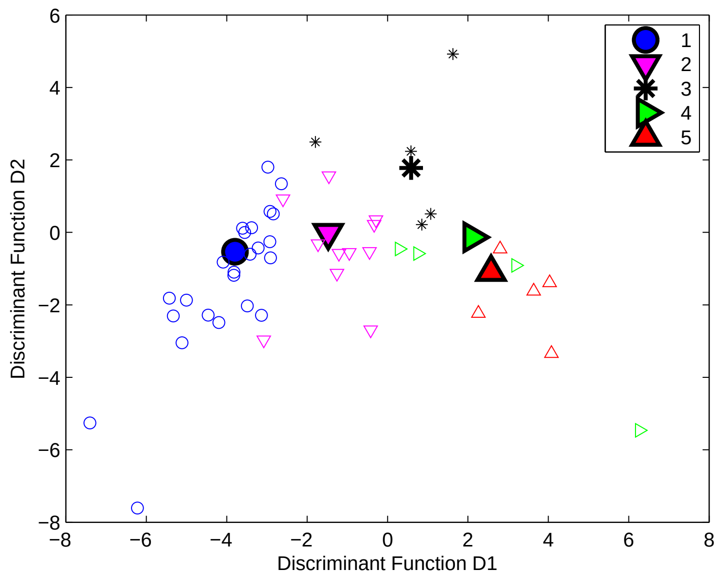

Figure 6.14: Combined Group Plots of Discriminant Functions 1 & 2 for R3-R2

Chapter 7

Conclusion and Future Work

7.1 Conclusion

The use of radio irregularity resulting from the movement of human objects crossing the path of a radio signal to detect human presence has been demonstrated previously and applied to intrusion detection [33, 34, 5]. However, the ability to detect more than one person remains a challenge if we rely on the characteristics of one signal's fluctuations. With pervasive networking brought about by large cyber-physical systems, the presence of numerous wireless communication devices allow us to study the fluctuations of multiple signals in close proximity of one another as a result of human interference and deduce the number of human objects that have crossed the paths of these signals.

In this thesis, we have provided studies on the characteristics of radio frequency, such as inter-packet interval, transmission power and wireless frequency channel, that could potentially affect the performance of detection. Then, we have proposed network-oriented approaches [4, 5, 6] that utilize received signal strength information (RSSI) of received packets to detect and count people when they cross the signal transmission paths. This information can be easily obtained from device drivers of wireless network interfaces when the packets are received and the goal of our approach is to be able to easily utilize the existing wireless transmitters and receivers already deployed in the environment. Our approach which is based on the RSSI fluctuations between consecutive packets does not require accurate channel models nor complex signal processing techniques. It only needs to be trained to detect the RSSI fluctuation patterns associated with the objects of interest, e.g. groups of different numbers of people; no additional tuning is required during deployment.

Using a simple configuration of two receivers deployed in close proximity to each other, we have first demonstrated the ability to detect two persons walking side-by-side along a typical 1.5m wide corridor using a straightforward approach based on the difference in the periods of fluctuations experienced by the two signals paths as the two human subjects pass. We then extended our scheme to detect more human subjects using the same two-receiver configuration together with discriminant analysis to process the signal fluctuation data; we validated our scheme in a controlled environment and showed that it is able to accurately detect and count up to five persons with an accuracy of almost 98%. Next, we deployed our scheme in a public area without the ability to control the mobility patterns and group structure of passerbys, and achieved comparable accuracy in counting people. However, we also note that a poorly located receiver can induce high estimation errors and significantly reduce the accuracy of the system. Ideally, a robust placement strategy should be chosen [35]. However, in our target scenario, achieving the best device placements from among the already deployed wireless devices may not always be possible. Additional wireless devices may need to be deployed to complement the existing topology, if the critical voids in detection are to be covered.

From this study, we conclude that a large cyber-physical system can be exploited for applications like people counting without the need for specialized hardware. However, our method is not aimed at completely replacing specialized hardware for automated people counting but more as a complementary technology. While the scheme in its current form requires further work to enhance its capabilities, it presents an exciting opportunity to turn an existing wireless communications network into a sensing system for automated people counting. The scenario that we have initially considered is a corridor-like space where it would be less cost effective to use more sophisticated systems, like imaging and thermal technology, yet is able to provide more information that the simple low-cost single-beam IR counter. Imaging would also be less effective as humans are blocked by one another from a camera located at one end of the corridor. There are many possible scenarios to be considered. Some of the questions that will be addressed as part of our ongoing and future work include the deployment scenarios of the proposed system and how it can complement other dedicated people counting technologies, without additional installation costs.

7.2 Future Work

7.2.1 Enhance Detection More People in A Group

In this thesis, we have demonstrated the ability to detect up to five people in a group using discriminant analysis. We also aim to improve the accuracy of detection of the maximum number of people in a group. This provides the potential to be able to apply the proposed people counting system to a wider area. We aim to look at different statistical methods that could provides better classification ability. The possible statistical methods are listed below.

- *Logistic Regression* [36] is used for predicting a limited number of categories based on predictor variables.

- *Naive Bayes Classifier* [37] is a popular classification method since it only requires a small amount of training data.

- *Decision Tree Learning* [38] is commonly used in machine learning which aims to predict the output based on several inputs using a tree model.

7.2.2 Automated People Counting in Outdoor Environment

We also aim to extend the scheme for automated people counting in outdoor environments, e.g., to count visitors in public parks [20], crowd size estimation [39], etc. Such technologies are increasingly being deployed for crowd size estimation to assist in crowd control and prevent any potential problems arising from loss of control over crowd size. Often, agencies involved in crowd safety and management require quick estimates to assist personnel on the ground, but most of the available technologies rely on image and video processing which are complex and expensive.

As our ongoing and future work, we are first extending the scheme for automated people counting in outdoor environments, i.e. to count visitors in public parks [40], and also adapting it for use in the monitoring of wildlife in natural habitats.

Appendix A

Data Analysis Process

We briefly outline the steps involved in processing the RSSI readings into statistical information and applying discriminant analysis to predict the number of people in a group.

A.1 Extracting Statistical Information

First of all, the positive detection is identified using the standard deviation detection approach. Statistical information is then extracted for each positive detection. The Matlab code in Table A.1 shows how the statistical information is extracted.

Mean and Standard Deviation The code in Table A.1 basically extracts the standard deviation of each positive detection and apply Matlab's built-in functions to calculated the mean and standard deviation of RSSI fluctuations. The coefficient of variation (CV) is then computed by dividing the standard deviation by the mean. R1_mean and R2_mean are the means of the positive detection for Receivers 1 and 2 respectively. R1_std and R2_std are the standard deviations of the positive detection for Receivers 1 and 2 respectively. indexA_1 and indexA_2 are the starting and ending index of a

Mean
R1_mean = mean(sig1(indexA_1:indexA_2)); R2_mean = mean(sig2(indexB_1:indexB_2));
Standard Deviation
R1_std = std(sig1(indexA_1:indexA_2)); R2_std = std(sig2(indexB_1:indexB_2));
Coefficient of Variation(CV)
R1_std = std(sig1(indexA_1:indexA_2)); R2_std = std(sig2(indexB_1:indexB_2));

Table A.1: Mean, Standard Deviation and CV Calculation

positive detection for Receiver 1 respectively while indexB_1 and indexB_2 are the index for Receiver 2.

Duration
R1_duration = indexA_2 - indexA_1; R2_duration = indexB_2 - indexB_1;
Area under the curve
R1_area = sum(sig1(indexA_1:indexA_2)); R2_area = sum(sig1(indexB_1:indexB_2));

Table A.2: Duration and Area Calculation

Duration and Area Similarly, the Matlab codes for computing the duration, which is the subtraction of the ending and starting index, and the area under the curve, the sum of standard deviation during each positive detection, are shown in Table A.2.

A.2 Applying Discriminant Analysis

With the statistical information extracted from the RSSI readings, we then use the SPSS statistical software [7] to perform discriminant analysis. There are two phases involved, namely, *training* and *classification*.

A.2.1 Training Phase

In the training phase, the number of people in a group is specified for each statistical information. Examples are shown in Table A.3 below. We then apply discriminant analysis to the statistical information using the SPSS statistical software with the commands shown in Table A.4. In the SPSS command, the number of people in a group from 1 to 5 is specified and discriminant analysis is applied to the independent variables to compute the discriminant functions and classification results of the training set which are shown in Tables 6.4 and 6.5.

A.2.2 Classification Phase

The classification of new cases can be done using SPSS based on the training cases (dataset(1)) as shown in Table A.5. The classification results of new cases is shown in Tables 6.6 and 6.7.

NPeople	R1_mean	R2_mean	R1_std	R2_std	R1_CV	R2_CV
1	2.1531	2.3685	0.1035	0.2203	0.0481	0.093
2	4.3969	4.9704	1.0649	0.8373	0.2422	0.1685
3	2.5052	2.9068	0.4375	0.5686	0.1746	0.1956
4	3.717	5.1933	1.0199	0.9306	0.2744	0.1792
5	3.6984	4.9782	1.3647	1.0823	0.369	0.2174

NPeople	R1_duration	R2_duration	R1_area	R2_area
1	10	9	47.7081	23.6847
2	12	10	102.6634	64.324
3	13	10	76.808	42.208
4	22	10	89.5948	101.5954
5	24	12	106.8216	99.7288

Table A.3: Examples of Statistical Information

```
DISCRIMINANT
/GROUPS=NPeople(1 5)
/VARIABLES=R1_mean R2_mean R1_std R2_std R1_CV R2_CV R1_duration
R2_duration R1_area R2_area
/ANALYSIS ALL
/PRIORS SIZE
/STATISTICS=MEAN STDDEV UNIVF BOXM COEFF RAW TABLE
/CLASSIFY=NONMISSING POOLED.
```

Table A.4: SPSS Discriminant Analysis Command

```
DISCRIMINANT
/GROUPS=NPeople(1 5)
/VARIABLES=R1_mean R2_mean R1_std R2_std R1_CV R2_CV R1_duration
R2_duration R1_area R2_area
/SELECT=datset(1)
/ANALYSIS ALL
/PRIORS SIZE
/STATISTICS=MEAN STDDEV UNIVF BOXM COEFF RAW TABLE
/CLASSIFY=NONMISSING POOLED.
```

Table A.5: SPSS Discriminant Analysis Command for New Cases

Bibliography

[1] P. Lee, W. Seah, H.-P. Tan, and Z. Yao, "Wireless sensing without sensors - an experimental approach," in *Proc. IEEE Int. Symp. on Personal, Indoor and Mobile Radio Communications(PIMRC 2009)*, pp. 62–66, Sept, 2009.

[2] P. Shankar, *Introduction to Wireless Systems*. New York: Wiley, 2001.

[3] I. Onat and A. Miri, "An intrusion detection system for wireless sensor networks," in *In Proceedings IEEE International Conference on Wireless And Mobile Computing, Networking And Commun. (WiCOM 2005)*, pp. 253–259, Aug, 2005.

[4] W.-C. Lin, W. Li, W. Seah, and T. Gulliver, "Inferring human activity using overcomplete dictionary based pattern recognition," in *2011 IEEE Pacific Rim Conference on Communications, Computers and Signal Processing (PacRim)*, pp. 155 –159, aug. 2011.

[5] W.-C. Lin, W. Seah, and W. Li, "Exploiting radio irregularity in the internet of things for automated people counting," in *2011 IEEE 22nd International Symposium on Personal Indoor and Mobile Radio Communications (PIMRC)*, pp. 1015 –1019, sept. 2011.

[6] W.-C. Lin, W. K. G. Seah, and W. Li, "People Counting using Radio Irregularity in Wireless Sensor Networks — Experimental Study," *ACM Transactions on Sensor Networks*, 2012. 1st revision submitted Aug 15, 2012.

[7] SPSS: An IBM Company, Homepage: http://www.ibm.com/software/analytics/spss/.

[8] E. Mathews and A. Poigne, "An echo state network based pedestrian counting system using wireless sensor networks," in *Proceedings of the International Workshop on Intelligent Solutions in Embedded Systems*, (Regensburg, Germany), pp. 1–14, 10-11 Jul 2008.

[9] Y. Zheng, D. J. Brady, and P. K. Agarwal, "Localization using boundary sensors: An analysis based on graph theory," *ACM Transactions on Sensor Networks*, vol. 3, Oct 2007.

[10] J. Nakamura, Y. Tomita, and S. Honda, "Algorithm for counting the number of persons using IR image processing," in *Proceedings of the IEEE Instrumentation and Measurement Technology Conference (IMTC)*, (Hamamatsu, Japan), pp. 220–223, 10-12 May 1994.

[11] Traf-Sys, "People Counting Systems." Homepage: http://www.trafsys.com.

[12] I. InfraRed, "Irisys – thermal technology for intelligent buildings." Homepage: http://www.irisys.co.uk.

[13] H. Celik, A. Hanjalic, and E. Hendriks, "Towards a robust solution to people counting," in *Proceedings of the IEEE International Conference on Image Processing (ICIP)*, (Atlanta, GA, USA), pp. 2401–2404, 8-11 Oct 2006.

[14] I. Amin, A. Taylor, F. Junejo, A. Al-Habaibeh, and R. Parkin, "Automated people-counting by using low-resolution infrared and visual cameras," *Measurement*, vol. 41, no. 6, pp. 589 – 599, 2008.

[15] CountWise, "People Counting Solution." Homepage: http://www.countwise.com.

[16] K. Woyach, D. Puccinelli, and M. Haenggi, "Sensorless sensing in wireless networks: Implementation and measurements," in *Proceedings of the 2nd International Workshop on Wireless Network Measurement (WiNMee)*, (Boston, MA, USA), Apr 2006.

[17] N. Patwari and J. Wilson, "RF Sensor Networks for Device-Free Localization: Measurements, Models, and Algorithms," *Proceedings of the IEEE*, vol. 98, pp. 1961–1973, November 2010.

[18] J. Wilson and N. Patwari, "Radio tomographic imaging with wireless networks," *IEEE Transactions on Mobile Computing*, vol. 9, pp. 621–632, 2010.

[19] N. Patwari and J. Wilson, "Spatial models for human motion-induced signal strength variance on static links," *IEEE Transactions on Information Forensics and Security*, vol. 6, pp. 791–802, Sep 2011.

[20] D. Puccinelli, A. Foerster, A. Puiatti, and S. Giordano, "Radio-based trail usage monitoring with low-end motes," in *Proceedings of the 7th IEEE International Workshop on Sensor Networks and Systems for Pervasive Computing (PerSeNS)*, (Seattle, WA, USA), 21 Mar 2011.

[21] W. Li and T. Gulliver, "Overcomplete dictionary based ultra-wideband signal detection," in *IEEE Wireless Communications and Networking Conference, 2006. (WCNC 2006).*, vol. 2, pp. 878 –883, April 2006.

[22] S. S. Chen, D. L. Donoho, Michael, and A. Saunders, "Atomic decomposition by basis pursuit," *SIAM Journal on Scientific Computing*, vol. 20, pp. 33–61, 1998.

[23] A. Antoniou and W.-S. Lu, *Optimization: Methods, Algorithms, and Applications*. Kluwer Academic Publishers, 2005.

[24] M. Nakatsuka, H. Iwatani, and J. Katto, "A study on passive crowd density estimation using wireless sensors," in *Proceedings of 4th International Conference on Mobile Computing and Ubiquitous Networking (ICMU)*, (Tokyo, Japan), 11-13 Jun 2008.

[25] MSP430, "Msp430 complete wireless development tool (ez430-rf2500) from texas instruments." Homepage: http://www.ti.com.

[26] Waspmote, "Waspmote wireless development board from Libelium." Homepage: http://www.libelium.com/products/waspmote.

[27] Simpliciti, "SimpliciTI Compliant Protocol Stack from Texas Instruments." Homepage: http://www.ti.com.

[28] Arduino, "Arduino is an open-source electronics prototyping platform." Homepage: http://www.arduino.cc/.

[29] G. J. McLachlan, *Discriminant Analysis and Statistical Pattern Recognition.*, vol. 35. John Wiley & Sons, Inc., 1993.

[30] R. A. Fisher, "The Use of Multiple Measurements in Taxonomic Problems," *Annals of Human Genetics*, vol. 7, no. 2, pp. 179–188, 1936.

[31] M. Welling, "Fisher Linear Discriminant Analysis." Class Notes, University of California, Irvine, CA, USA, 2005.

[32] R. B. Burns and R. A. Burns, *Business Research Methods and Statistics Using SPSS.* SAGE publication Ltd., 2008.

[33] P. Lee, W. K. G. Seah, H. P. Tan, and Z. Yao, "Wireless Sensing Without Sensors – An Experimental Study of Motion/Intrusion Detection using RF Irregularity," *Measurement Science and Technology, Special Issue on Wireless Sensor Networks: designing for real-world deployment and deployment experiences*, vol. 21, Nov 2010.

[34] M. Youssef, M. Mah, and A. Agrawala, "Challenges: device-free passive localization for wireless environments," in *Proceedings of the 13th Annual ACM International Conference on Mobile Computing and Networking*, (Montréal, QC, Canada), pp. 222–229, 9-14 Sep 2007.

[35] A. Krause, C. Guestrin, A. Gupta, and J. Kleinberg, "Robust sensor placements at informative and communication-efficient locations," *ACM Transactions on Sensor Networks*, vol. 7, pp. 31:1–31:33, Feb 2011.

[36] A. Agresti, *Categorical Data Analysis*. Wiley Series in Probability and Statistics, Wiley-Interscience, 2nd ed., 2002.

[37] E. Frank and R. R. Bouckaert, "Naive bayes for text classification with unbalanced classes.," in *PKDD* (J. Fürnkranz, T. Scheffer, and M. Spiliopoulou, eds.), vol. 4213 of *Lecture Notes in Computer Science*, pp. 503–510, Springer, 2006.

[38] J. R. Quinlan, "Induction of decision trees," *Mach. Learn.*, vol. 1, pp. 81–106, Mar. 1986.

[39] Y.-L. Hou and G. Pang, "Automated people counting at a mass site," in *Proceedings of the IEEE International Conference on Automation and Logistics (ICAL)*, (Qingdao, China), pp. 464–469, 1-3 September 2008.

[40] GreenSpace, "A guide to automated methods for counting visitors to parks and green spaces."